The role of matricellular proteins Nov and Wisp1 in aging and myocardial infarction

By

Danielle Giroux

This thesis is submitted to the Faculty of Graduate and Postdoctoral Studies in partial fulfillment of the requirements for the Degree of:

Master of Science in Cellular and Molecular Medicine

Department of Cellular and Molecular Medicine

Faculty of Medicine

University of Ottawa

Division of Cardiac Surgery

University of Ottawa Heart Institute

Abstract

Background. The **C**ysteine-rich protein, **C**onnective tissue growth factor, and **N**ephroblastoma overexpressed protein (CCN) family of matricellular proteins are signaling molecules found in the extracellular space, which can have pro-angiogenic, anti-inflammatory and anti-fibrotic properties. Their expression and role in repair and remodeling after myocardial infarction (MI) remains to be better elucidated. In this study, the age-associated expression of Nov (CCN3) and Wisp1 (CCN4) were examined post-MI in mice. **Methods and Results.** *In vivo*, MI was induced in young (6 week) and old (12-14 months) mice. Cardiac function was assessed by echocardiography, showing that LVEF was reduced in old mice (33.9%) at 14 days post-MI compared to young mice (43.9%; p=0.002). RT-qPCR analysis of harvested myocardial tissue revealed that mRNA expression of several matricellular proteins in healthy tissue was decreased by 2.5- to 5-fold in old compared to young mice (p=0.03 for Nov, p=0.04 for Wisp1, p=0.0002 for TnC, p=0.04 for TSP-1). Post-MI, mRNA expression of Nov was reduced in the infarct (by up to 13-fold; $p\leq0.03$) and border zone (by up to 16-fold; $p\leq0.002$) in old compared to young mice. Nov and Wisp1 protein expression was also reduced in old compared to young mice in the infarct and border zones; specifically, for Nov in the infarct zone (p=0.01) and the border zone (p=0.009) at 2 days post-MI and for Wisp1 in the infarct zone at 2 days (p=0.0003) and 14 days (p=0.003), along with 7 days post-MI in the border zone (p=0.0003). To identify possible sources of matricellular proteins, *in vitro* culture experiments were performed. The expression of Nov protein was increased (1.9-fold; p=0.006) in TGF-β stimulated cardiac fibroblasts after 48h, as was the expression of the myofibroblast marker α-SMA (1.7-fold; p=0.035). Wisp1 mRNA expression was increased (4.5-fold; p=0.03) in stimulated cardiac fibroblasts after 48h in a hypoxic environment. There was also a trend for increased mRNA expression of Nov (p=0.118)

and Wisp1 (p=0.121) in M2 macrophages. Cardiac fibroblasts treated with Nov+TGF-β exhibited greater proliferation (by 29%; $p \leq 0.01$), as did those treated with Wisp1+TGF-β (by 16%; $p \leq 0.05$). Treatment with Nov or Wisp1 led to an increase in viability of cardiac fibroblasts both in the presence (Nov; p=0.0004, Wisp1; p=0.01) and absence of TGF-β (Nov; p=0.0005, Wisp1; p=0.003). **Summary.** There is an age-associated difference in the expression of matricellular proteins Nov and Wisp1 between both healthy and MI mice. *In vitro* studies suggest that cardiac fibroblasts may produce Nov and Wisp1 upon their activation to myofibroblasts. The presence of these proteins was also shown to increase the proliferation and viability of fibroblasts. Therefore, reduced levels of Nov and Wisp1 in old mice may negatively affect the repair and remodeling process post-MI compared to young mice. A better understanding of Nov and Wisp1 function in aging and post-MI repair may help identify novel therapeutic targets for limiting damage post-MI and improving repair and heart function.

Table of Contents

List of Figures

List of Tables

List of Abbreviations

Alpha-Smooth Muscle Actin	α-SMA
Bone Marrow Derived Macrophages	BMDM
Bone Morphogenic Protein	BMP
Bovine Serum Albumin	BSA
Cardiovascular Disease	CVD
Cysteine-rich protein, Connective Tissue Growth Factor, Nephroblastoma overexpressed protein	CCN
Connective Tissue Growth Factor	CTGF
Deoxyribonucleic Acid	DNA
Dithiothreitol	DTT
Dulbecco's Modified Eagle Media	DMEM
Extracellular Matrix	ECM
Ethylenediaminetetraacetic Acid	EDTA
Hanks Balanced Salt Solution	HBSS
Heart Failure	HF
Histone Deacetylase	HDACs
Interleukin	IL
Left Anterior Descending	LAD
Left Ventricle	LV
Left Ventricular Ejection Fraction	LVEF

Matrix metalloproteinase	MMP
MicroRNA	miRNA
Myocardial Infarction	MI
Nephroblastoma over expressed protein	Nov
Nucleoside Triphosphate	dNTP
Paraformaldehyde	PFA
Reactive Oxygen Species	ROS
Ribonucleic Acid	RNA
Tenacin-C	TnC
Tissue Inhibitor of Metalloproteinase	TIMP
Transforming Growth Factor-Beta	TGF-β
Thrombospondin-1	TSP-1
Tumor Necrosis Factor-alpha	TNF-α
Vascular Smooth Muscle Cells	VSMC
Wnt-inducible secreted protein-1	Wisp1

Acknowledgements

To start, I would like to thank all the members of the Suuronen lab who I have had the pleasure to work with. I would like to thank Dr. Brian McNeill, Dr. Branka Vulesevic and Dr. Nicholas Blackburn whom were always available for guidance, assistance and contributed to my development as a graduate student. Especially Brian, I would not have been able to complete my studies without your motivation and direction to further my project. Furthermore, my fellow graduate students; Çagla Eren, Mayté Gonzalez-Gomez, Veronika Sedlakova, Justina Pupkaite and Godwin Dogbevia. I will forever cherish the many memories and laughs we have had together through our time studying. You are some of the kindest and most thoughtful people have I ever met. Your loving hearts will always be with mine no matter where we are in the world.

To Suzanne Crowe, thank you for arranging my training for the lab, while making me feel welcome to the Suuronen team. Your patience and organizational skills have been a great help throughout my studies. A special thanks to Rick Seymour and the animal care team at the University of Ottawa Heart Institute for their help with all animal care and procedures.

I would like to thank my family and friends for their support during these past two years. I am so grateful to have you helping me along the way and giving me company on weekends to distract me from all my lab work. To Madison McNutt, you have been my shoulder to lean on through the completion of my Master's. I don't know if I'll ever be able to thank you enough for your continuous support, motivation and ability to make me laugh through all of the ups and downs.

My gratitude goes out to my thesis advisory committee; Dr. Wenbin Liang and Dr. Patrick Burgon for their guidance and help with advancing my project. All of your comments and questions throughout my progress are appreciated. Your valuable advice helped immensely with the final outcome of my project.

Finally, I would like to thank my supervisor Dr. Erik Suuronen for accepting me to be a part of his lab. My time here has allowed me to gain knowledge in cardiovascular research and achieve valuable skills in the laboratory setting that I will be able to use for the rest of my life journey. Without Erik I would not have been able to accomplish any of this and I'm very thankful to have had the opportunity to have him as a supervisor.

None of this would have been possible without any of you.

List of Contributions

Lab training and technical support was provided by various members of the Suuronen lab. Funding of this project was made possible because of Dr. Erik Suuronen, Dr. Marc Ruel and Dr. Emilio Alarcon. Dr. Erik Suuronen was responsible for the design and organization of this project. The animal surgeries were performed by of Rick Seymour and the University of Ottawa Animal care team was responsible for the maintenance of all animals used throughout the study.

Introduction

1. Introduction

1.1. The Aging Cardiovascular System

Cardiovascular disease (CVD) is the leading cause of morbidity and mortality globally. It is defined as a condition with impaired physiological function of the heart and blood vessels (Thygesen, Alpert, & White, 2007). There are multiple risk factors associated with CVD including genetic predisposition, diabetes, race, smoking, obesity, hypertension and age (Elias, Elias, Sullivan, Wolf, & D'Agostino, 2005). Prolonged risk factors associated with CVD can often lead to occlusions in the vasculature causing cardiovascular related complications such as acute myocardial infarctions (MI), eventually leading to heart failure (HF) (Paneni, Canestro, Libby, Luscher, & Camici, 2017). Although many of these risk factors can be controlled or altered, aging however, is inevitable. CVD has the greatest burden on elderly populations, with 90% of all HF deaths occurring in individuals over the age of 70 (Strait & Lakatta, 2012). This is in part due to the increased risk for developing CV related complications through structural and functional alterations that accumulate throughout life, and the increase in the aged population worldwide, due to better preventive and medical care (Stewart, 2003; Strait & Lakatta, 2012). With the incidence of CVD expected to rise to 43.9% in the adult population of the United States by 2030 (Benjamin et al., 2017), there is an interest in determining the effects of aging on the normal cardiovascular system as well as those that are amplified following a CVD-associated event. For instance, there are structural and functional changes, alterations to the repair mechanisms, and systemic organ changes (Strait & Lakatta, 2012)(Meschiari, Ero, Pan, Finkel, & Lindsey, 2017). Age-related changes that accumulate from early life are thought to alter

vascular function, yet, aging itself will only lead to moderate impairment of myocardial function without a previous CV related complication (Paneni et al., 2017; Strait & Lakatta, 2012).

The heart supplies the body with oxygen rich blood, which also delivers nutrients and removes waste around the body. The cardiac muscle is unique in that it lacks the ability to regenerate after injury (Talman & Ruskoaho, 2016). It also has a limited ability to repair the structural and functional changes that occur in the aging heart. This leads to changes in the size of the cardiomyocytes and the shape of the heart to a more spheroid figure after an increase in myocardial wall thickness (Strait & Lakatta, 2012). Additionally, there is an increase in collagen tissue deposition in the ventricles, increasing ventricular stiffness (Gazoti Debessa, Mesiano Maifrino, & Rodrigues de Souza, 2001). Consequently, the overall change in structure with aging affects the contractile efficiency, increasing stress within the heart, resulting in an increased health burden on the aging populations. These age-related changes to the heart increase the likelihood of cardiovascular related complications in the aged populations and their susceptibility to an acute MI. MI is considered one of the most powerful risk factors leading to HF, and the incidence of HF is expected to increase (Meschiari et al., 2017). Therefore, further understanding of the epidemiology and treatments for MI may help the outcomes following a CV-related event, particularly in the aging population.

1.2. Cardiac Repair and Remodeling Post-MI

In the event of a myocardial infarction (MI), the adult mammalian heart lacks the ability to regenerate to its full capacity. This leads to adverse remodeling of the myocardium, resulting in structural and functional alterations. Adverse cardiac remodeling is commonly associated with the progression of HF. Following an ischemic injury, there are three complex overlapping phases

which occur in an attempt to preserve cardiac function: The Inflammatory, Proliferative and Maturation phases (Fig. 1). Understanding these phases is of importance in the attempt to optimize cardiac repair following an ischemic event and limit adverse remodeling that may lead to ventricular dilation, loss of structural integrity and decreased function.

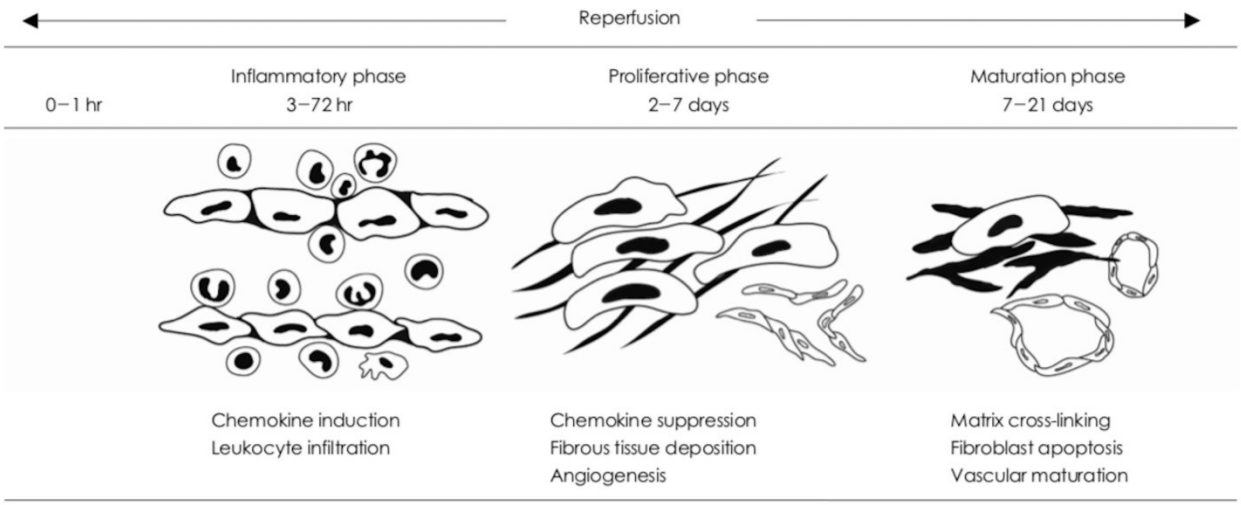

Figure 1. The Three Overlapping Healing Phases Post-MI in Mice. Upon injury, the heart undergoes a repair and remodeling process in an attempt to restore structure and function. Since the heart has limited regenerative capabilities, the lost cardiomyocytes are not replaced, but rather inflammation leads to fibrosis and scar formation to reinforce the myocardial wall (Nah & Rhee, 2009).

1.2.1. The Inflammatory Phase

Directly following an ischemic event, the inflammatory response is triggered, peaking at 3-72 hours post-MI in mice. In the infarcted myocardium there is an accumulation of reactive oxygen species (ROS) from increased oxidative stress that coexists with apoptosis (Frangogiannis, 2014). Many cell types including inflammatory leukocytes (neutrophils and mononuclear cells), endothelial cells, and other noncardiomyocytes are recruited to the infarct area, triggering an inflammatory cascade that results in healing and the replacement of the damaged myocardium and dead cardiomyocytes (Frangogiannis, 2014; Nah & Rhee, 2009).

Moreover, research has revealed a function for the canonical Wnt signaling pathway for mediating inflammatory responses after its activation in response to cardiac injury (Bergmann, 2010; W. Fu, Wang, & Zeng, 2018). The lack of oxygen causes myocyte apoptosis and cell necrosis, with increased expression of caspase 3 (Krijnen et al., 2002) . Caspases play a key role in the process of apoptosis and their overexpression has been related to depressed cardiac function (Krijnen et al., 2002). In order to remove these necrotic and apoptotic cells, the reparative response triggers pro-inflammatory signals through cytokine and chemokine induction and leukocyte infiltration via a positive-feedback loop in the neighboring normal myocardium. In this state, TNF-α and IL-1β stimulate an increase in cellular adhesion molecules and subsequent infiltration of inflammatory cells, thereby increasing phagocytic macrophage numbers to remove cardiomyocytes undergoing apoptosis and necrosis, as well as other types of cellular debris (De Haan, Smeets, Pasterkamp, & Arslan, 2013; Nah & Rhee, 2009). Macrophages are the main immune cells in cardiac repair following ischemia with the ability to be polarized to a pro- or anti-inflammatory phenotype, thereby regulating many reparative and regenerative roles.

1.2.2. Macrophages in Post-MI Repair

The immune system facilitates scar formation in the myocardium post-MI with its initial inflammatory response following injury. Of importance is the monocyte/macrophage population of cells since they are capable of secreting factors that facilitate remodeling of the LV, depending on their polarization phenotype, thereby altering their function. Hence macrophages have the ability to control the inflammatory and reparative functions post-MI. There are subpopulations of macrophages based on their expression of multiple markers, indicating their polarization: M0, M1, or M2. M0 macrophages are thought to be unpolarized macrophages that have the ability to

differentiate based on external factors in their local environment (Lindsey, Saucerman, & DeLeon-Pennell, 2016). However, following inflammation, the pro-inflammatory/M1 phenotype population increases in the presence of pro-inflammatory cytokines, e.g. IL-1β and TNF-α, which phagocytose apoptotic and necrotic bodies (Hulsmans, Sam, & Nahrendorf, 2016). This correlates to reduced collagen synthesis and increased ECM degradation through an increase in Matrix Metalloproteinase (MMP) expression (Frangogiannis, 2014). Once apoptotic cells are removed, there is an increase in anti-inflammatory cytokines produced by cells including macrophages (Hulsmans, Sam, & Nahrendorf, 2016), and fibroblasts (Chistiakov, Orekhov, & Bobryshev, 2016), promoting the transition to the tissue healing phase. Fibroblasts are recruited to the area, stimulating a transition from the inflammatory phase to the proliferative phase, where there is a changeover from M1 macrophages to M2/anti-inflammatory macrophages.

The M2 subpopulation are thought to be reparative macrophages, producing IL-10 and TGF-β, cytokines needed throughout the proliferative and maturation phase of cardiac remodeling (Hulsmans, Sam, & Nahrendorf, 2016). However, prolonged activation of the M2 phenotype has been shown to contribute to cardiac fibrosis, causing ventricular stiffness due to their ability to activate fibroblasts (Leor, Palevski, Amit, & Konfino, 2016). Given their various roles in cardiac remodeling, their roles are of particular interest in aging.

In the neonatal mouse heart, there is evidence indicating the important function of macrophages for driving angiogenesis and tissue regeneration following MI (Aurora et al., 2014). Additionally, they have a dynamic role in an infarct environment mediating the inflammatory responses. In inflammation with cardiac aging, macrophage levels are increased in the LV and polarization to M1 vs M2 is also altered. This ratio consequently affects the

reparative process post-MI, demonstrating an additional interest in how the M1 and M2 phenotypes affect the repair and remodeling process of the heart post-MI.

1.2.3. The Proliferative Phase

The proliferative phase peaks at 2-7 days post-MI in mice, with the induction of anti-inflammatory cytokines in the myocardium from various cell types. Additionally, there is a continuation of leukocyte recruitment and inflammation, while macrophage subpopulations secrete growth factors and pro-fibrotic cytokines like TGF-β. TGF-β synthesis is consistently upregulated in many animal models of MI, indicating its critical role in cardiac injury, repair and remodeling (Dobaczewski, Chen, & Frangogiannis, 2011; Nah & Rhee, 2009). Its upregulation causes the recruitment of proliferating cardiac fibroblasts, stimulating ECM protein synthesis and increasing cardiomyocyte hypertrophy, with fibrosis as the outcome (Dobaczewski et al., 2011; Shinde & Franogogiannis, 2014). The increase in TGF-β additionally causes an rise in fibroblast number in the heart from local recruitment, circulating progenitor cells, as well as vascular cells to initiate pro-angiogenic pathways for revascularization (Dobaczewski et al., 2011). This demonstrates its key role in the proliferative phase post-MI.

Within the first 2-4 days of the proliferative phase, fibroblasts are highly proliferative and actively secreting growth factors and signaling molecules to assist in the reparative phase. The proliferating fibroblasts are then activated to myofibroblasts at days 3-7, expressing smooth muscle-like properties (X. Fu et al., 2018). These myofibroblasts cells deposit the bulk of ECM proteins responsible for preserving the structural integrity of the ventricle by matrix protein synthesis; particularly collagen. However, at this stage many other regulatory proteins are also secreted, such as the matricellular proteins for modulating cellular and molecular signals in

response to injury. Of importance is the regulation of endothelial cells and capillary network formation to promote angiogenesis and the reperfusion of the infarcted area. Angiogenesis is a highly important part of the healing process since without vascularization the tissue would be hypoxic (Prabhu & Frangogiannis, 2016). This process is highly dependent on the extracellular environment cues during stress and the function of MMPs to degrade the ECM and promote endothelial cell migration (Souders, Bowers, & Baudino, 2009). Therefore, the cardiac ECM plays a fundamental role in the proliferative phase in restoring blood flow to the location of injury in the heart tissue to limit its loss of function.

1.2.4. The Maturation Phase

The deposition of ECM proteins begins the formation of the collagenous scar in the infarct area. At this phase there is a decreased level of cardiomyocytes and increased amount of fibroblast apoptosis in the infarct and border zones (Lajiness & Conway, 2014; Van Linthout, Miteva, & Tschöpe, 2014). These cellular components are replaced by an intricate collagen-based scar formed from the crosslinking of the deposited cardiac matrix, initiating the maturation phase. Additionally, the canonical and non-canonical Wnt pathways have been shown to contribute to the regulation of cardiac fibroblasts, promoting myofibroblast differentiation and cardiac fibrosis (W. Fu et al., 2018; Meyer et al., 2017). This complete repair response post-MI renders the heart with reduced cardiac function and increased tissue stress due to the rigidity of the scar and its inability to contribute to a synchronous heart beat (St. John Sutton & Sharpe, 2000). After 14-28 days in mice, excessive fibrosis can be seen, with amplified cardiomyocyte hypertrophy, thereby increasing left ventricular dilation and, in some cases, leading to HF. Consequently, the maladaptive remodeling of the ECM and extracellular signals may be related,

in part, to the ECM proteins during the remodeling process, including matricellular protein functions. If we can control the mechanistic properties of the ECM and its corresponding proteins involved in tissue repair and remodeling, we may be able to ameliorate cardiac function post-MI. Therefore, more background information on fibroblasts, the cardiac ECM and matricellular proteins will be described in the following sections.

1.2.5. Fibroblasts in Post-MI Repair and Remodeling

Cardiac fibroblasts are one of the most abundant cell types in the myocardium, and the primary source for the generation of collagens I, III and IV, matricellular proteins, fibronectin, integrins, MMPs and TIMPs, and many other components of the ECM (Barbara, 2016). Under normal physiological conditions, fibroblasts are responsible for ECM homeostasis and providing a scaffold for cardiomyocytes to help maintain cardiac structure and coupling of the electrical signaling. Following an MI, the resulting mechanical stress, TGF-β secretion and altered ECM homeostasis causes a change in the phenotype of cardiac fibroblasts, thus increasing ECM protein deposition in the myocardium (Furtado, Nim, Boyd, & Rosenthal, 2016; Van Linthout et al., 2014). These proteins are secreted by activated and proliferating fibroblasts; termed myofibroblasts, which are the major producers of ECM proteins and collagen. The TGF-β regulated transdifferentiation of fibroblasts to myofibroblasts is an important event in the proliferative phase of cardiac remodeling, leading to reparative fibrosis (Van Linthout et al., 2014). Additionally, the expression of α-SMA and other contractile proteins are markers of activated myofibroblasts, demonstrating their contractile ability, attempting to maintain cardiac function in the LV (Fang, Murphy, & Dart, 2017; Weber, Sun, Bhattacharya, Ahokas, & Gerling,

2013). Myofibroblasts are essential for maintaining ECM balance and providing a contractile phenotype for maintaining structural function.

During the final phases of the repair and remodeling process post-MI, it has been noted that fibroblasts have the ability to differentiate again into another phenotype known as matrifibrocyte (X. Fu et al., 2018). This cell lacks the contractile protein α-SMA, but it is highly specialized for a collagen-rich environment, expressing unique ECM genes for maintaining the mature collagen scar that forms in the myocardium post-MI (X. Fu et al., 2018). However, evidence has also suggested that as the scar matures, the number of myofibroblasts decreases and are eventually cleared through apoptosis or other forms of cell death (W. Chen & Frangogiannis, 2013; Fan, Takawale, Lee, & Kassiri, 2012). This may be a result of reduced growth factor secretion and matricellular protein function that deprive the activated fibroblasts of pro-survival and proliferative abilities. Yet, too much apoptosis may lead to negative fibrosis within the myocardial walls and infarct expansion (Fan et al., 2012). In summary, there are many phenotypes responsible in post-MI LV remodeling of the myocardium and an enhanced understanding of the cell source and regulatory mechanisms may facilitate the identification of potential new therapeutic targets in ischemic injury.

1.3. The Cardiac ECM

The cardiac ECM plays an important role in the healthy and injured heart. Maintaining ECM homeostasis is essential for structure and function, however upon injury the balance of ECM deposition and degradation is altered. With inflammation, the increase in pro-inflammatory cytokines stimulates an increase in MMP production, degrading the cardiac ECM, and the induction of inhibitory cytokines enhances matrix deposition with increased Tissue inhibitor of

metalloproteinase (TIMP) expression (Bonaventura, Montecucco, & Dallegri, 2016; Dobaczewski, Gonzalez-Quesada, & Frangogiannis, 2010; Ma et al., 2014). The majority of ECM proteins are deposited following infarction to replace dead myocytes in an attempt to maintain structural integrity. MMP-2 and MMP-9 play an important role in degrading the ECM, thereby generating matrix fragments which are essential for immune cell recruitment to clean the area of debris. Recruited cells can then adhere to the ECM, release growth factors and signals to other cells within the ECM to mediate repair (De Haan et al., 2013). These ECM cellular signals and cell-cell interactions are key to activating TIMPs and allowing for the transition from the inflammatory to proliferative phases.

In the proliferative phase, the transdifferentiation of fibroblasts to active myofibroblasts leads to the increased ECM deposition. Activated fibroblasts are responsible for secreting ECM proteins like matricellular proteins and growth factors to modulate the inflammatory and reparative phases. Additionally, the cardiac ECM fills the gaps between the cells to maintain structural integrity of the ventricle, preventing further damage and limiting functional loss (Bonaventura et al., 2016). This comprises an increase in ECM proteins and collagen content to initiate scar formation, and the production of matricellular proteins for regulating inter- and intra-molecular signals and cytokines to recruit cells responsible for initiating reperfusion of the infarcted area and begin angiogenesis (Bonaventura et al., 2016; Souders et al., 2009). Therefore, the cardiac ECM plays a significant role in the proliferative phase.

The maturation phase begins with the increase in ECM protein deposition like collagen type I and III to produce the dense scar (Chistiakov et al., 2016; Furtado et al., 2016). This is marked by the cross-linking of the new cardiac ECM to form the mature scar, with an altered ECM architecture. The scar provides tensile strength to the ventricle in an attempt to preserve

cardiac function (Dobaczewski et al., 2010). However, excess cross-linking of the ECM causes ventricular stiffening, ventricular dilation and excessive fibrosis, which can ultimately lead to heart failure. Looking at some of the key proteins within the ECM like matricellular proteins may be of interest in understanding their functions and regulatory abilities post-MI.

1.4. Matricellular Proteins

Matricellular proteins are non-structural components within the ECM with many functions including: regulating cell-matrix and cell-cell interactions, and exerting many direct and indirect functions on cellular phenotype and growth factor-mediated responses (Bornstein, 2009). Their expression is generally elevated during embryogenesis and in adulthood in response to injury (Schellings, Pinto, & Heymans, 2004). They have various roles in cell signaling, death, communication, adhesion, differentiation and survival, with expression in many tissue and cell types through cell surface receptor binding. They have been shown to be upregulated in fibrotic diseases and in the presence of tissue damage (Leask & Abraham, 2006; B. Perbal, 2018). Additionally, several families of matricellular protein have been shown to have increased expression and function in the myocardium post-MI and in response to injury, such as tenascin-C, thrombospondin, and the osteopontin and CCN family of matricellular proteins (Bornstein, 2009; Franogogiannis, 2011; Schellings et al., 2004). However, their exact mechanism and how they interact with different cell types is not fully understood. Based on the evidence gathered so far, they are of interest in studying the cardiac ECM and its repair and remodeling post-MI.

1.4.1. The CCN Family of Matricellular Proteins

The CCN (**c**ysteine-rich protein (Cry61), **C**onnective tissue growth factor (CTGF), **N**ephroblastoma overexpressed protein (Nov)), family of matricellular proteins consists of six, structurally similar, highly conserved and biologically distinct members who play major roles in many fundamental biological processes including development, response to injury, wound repair and fibrosis (A. Perbal & Perbal, 2016; B. Perbal, 2018; Twigg, 2018; Yeger & Perbal, 2016). The family is named after the first three members identified, while a few years later the last three proteins were found –Wnt-inducible secreted protein 1-3 (Wisp1/CCN4, Wisp2/CCN5, and Wisp3/CCN6). The CCN family shares the same conserved tetra-modular structural composition, providing the basis for diverse biological functions each of these proteins possess. This is due to the potential binding abilities of each domain and their ability to bind to various proteins and ligands, exerting many biological functions (Fig. 2). It should be noted that these CCN proteins are associated within the ECM, possessing regulatory roles with little to no structural functions. Amongst these roles are cell growth, differentiation, development, adhesion, communication and signaling (B. Perbal, 2018).

Recent research has demonstrated a role for the CCN family of matricellular proteins in tissue repair, making them of interest in cardiac repair and remodeling post-MI. Their expression in the infarct area following injury is tightly regulated by various growth factors and signaling molecules such as TGF-β. This allows their integration into the ECM via integrins, heparin sulphated proteoglycans (HSPGs), fibronectin, LDL receptor protein-1 (LRP-1) and collagen V interactions and binding to elicit their specific cellular signals to transduce their effects on cells responsible for the repair process (Fig. 2) (Frangogiannis, 2011). Studies have identified that each member of the CCN family can target multiple cell receptors due to their ability to bind to

multiple binding partners. However, CCN binding is largely dependent on the cell and tissue type, contributing to their varying roles, rendering them of interest in cardiac repair and remodeling post-MI.

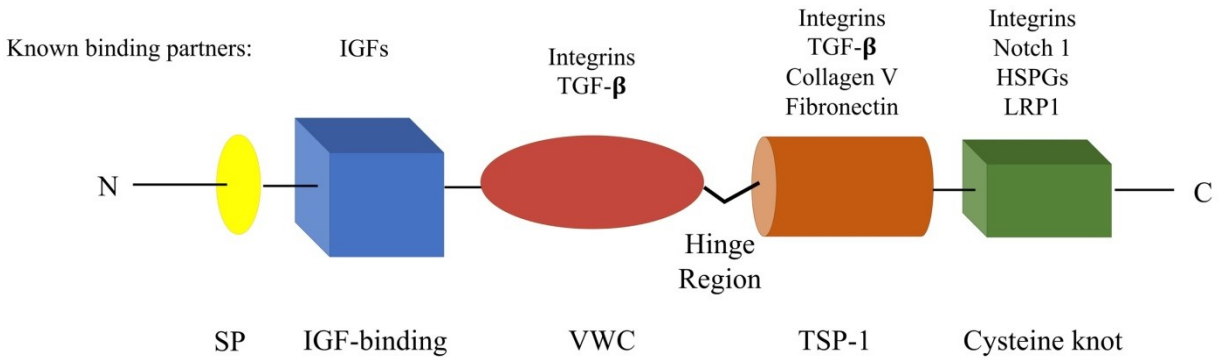

Figure 2. The Conserved Structure of the CCN Family of Matricellular Proteins. Each of the family members contain multiple domains linked by a variable hinge region: a signal peptide (SP), insulin-like growth factor (IGF)-binding domain, a von Willebrand type C domain (VWC), a thrombospondin type-1 repeat (TSP-1) and a cysteine knot, all capable of binding to multiple proteins, ligands and receptors such as integrins, TGF-β, heparin sulphated proteoglycans (HSPGs), fibronectin, LDL receptor protein-1 (LRP-1), collagen V, Notch 1.

The CCN family of matricellular proteins is of interest in cardiac repair and remodeling due to their recently discovered roles in response to cardiac injury. For example, CCN1/Cry61 has been shown to regulate some events during the inflammatory response through cell adhesion, migration and proliferation in the myocardium (Bai, Chen, & Lau, 2010), while together CCN1 and CCN2/CTGF have been shown to be involved in inducing angiogenesis in the cardiovascular system through various integrin binding sites, which are specific to the cell types (Lau, 2012). Furthermore, our lab has demonstrated the use of CCN1 to interact with integrins specific to enhancing pro-survival and pro-angiogenic genes with the use of cell-matrix interactions post-MI (McNeill, Vulesevic, Ostojic, Ruel, & Suuronen, 2015). Yet, there is limited knowledge on the functions of other CCN members in the myocardium (further described in the following

sections). With the understanding that the cardiac ECM is altered with age, it is likely that the secretion and function of matricellular proteins in involved, thereby also affecting their role post-MI in the aged myocardium.

1.4.2. CCN Protein Nov/CCN3

Currently, few functions of CCN3 in the myocardium are known; however, it is proposed to promote angiogenesis, with anti-fibrotic properties in many other tissues (Borkham-kamphorst, Roeyen, & Leur, 2012; C. G. Lin, Chen, Leu, Grzeszkiewicz, & Lau, 2005; Marchal et al., 2015). Research has showed that CCN3 promotes cell adhesion and survival in endothelial and fibroblast cells through multiple integrin cell surface receptors in wound healing, resulting in enhanced angiogenesis (C. Lin et al., 2003). Furthermore, increased CCN3 mRNA expression has been observed in the kidney and liver in a diabetic mouse model, and this correlated inversely to the amount of fibrosis observed (Borkham-kamphorst et al., 2012). It has also been noted that CCN3 levels are increased 5-7 days post-tissue injury, leading to reduced pro-inflammatory cytokine expression in Chronic Kidney Disease models (Franogogiannis, 2011; Lin et al., 2005; Marchal et al., 2015). Moreover, much research has been completed demonstrating that Nov elicits its functions through integrins and the Notch signaling pathway, modifying signaling responses, with their physiological effects depending on their interactions (C. G. Lin et al., 2005; Ren et al., 2014; Wolf et al., 2010). Nov also has the ability to bind many ECM proteins, cytokines and growth factors in other tissues that are known to be upregulated in the myocardium post-MI, such as TGF-β (Liu et al., 2017). This suggests specific interactions for Nov in wound healing and may provide an insight in the cardiac remodeling process post-MI. For example, its pro-angiogenic properties during other tissue repair, may translate to functions

in the heart and the knowledge that Nov is present in many fibrotic diseases makes it a key target in post-MI repair and remodeling perhaps regulating cardiac fibrosis and scar formation.

1.4.3. CCN Protein Wisp1/CCN4

Wisp1 (CCN4) is a downstream mediator of the Wnt signaling pathway, known to be upregulated during embryogenesis and in many fibrotic disorders (Königshoff et al., 2009; Stephens et al., 2015). Recent evidence suggests that Wisp1 expression is elevated post-MI, localizing primarily to the infarct zone and surrounding myocardium (Franogogiannis, 2011; Venkatachalam et al., 2009), particularly at 7 days post-MI (Colston et al., 2007). However, its exact mechanisms have yet to be elucidated. Since the Wnt signaling pathways is essential in organ development in embryos (Königshoff et al., 2009), it also suggests a role in tissue repair through the upregulation of Wisp1, particularly in cardiac remodeling following an acute MI. At the site of injury, it has been suggested that Wisp1 promotes the proliferation of fibroblasts, with pro-survival functions through the canonical and non-canonical Wnt signaling pathways via TNF-α activation *in vitro* (Bergmann, 2010; Meyer et al., 2017). Furthermore, it has been shown to have the ability to activate pro-angiogenic pathways in lung, colon and breast endothelial and fibroblast cells (Bergmann, 2010; C. C. Chen & Lau, 2009; Stephens et al., 2015). Altogether, these findings suggest a possible role for Wisp1 in cardiac remodeling post-MI. It has also been shown that Wisp1 can stimulate cardiomyocyte hypertrophy and enhance ECM deposition *in vitro,* however these functions are yet to be reported *in vivo* (Colston et al., 2007). These known functions insinuate a role for Wisp1 in post-MI remodeling. Therefore, if we can gain an understanding of some of the functions and properties of Wisp1 in the post-MI myocardium *in*

vivo, it may provide an approach to enhance post-MI outcomes in the aging population who have reduced cell and tissue function.

1.5. The Aging Cardiac ECM

With aging, human physiology changes and the cardiac myocardium undergoes structural and functional alterations. This leads to a decline in overall myocardial performance. The cardiac ECM plays an important role in maintaining structural geometry of the heart and modulating many cellular signals. Therefore, ECM homeostasis is important to maintain for proper cardiac function. Many of the changes that occur with aging results in increased left ventricular wall stress which leads to cardiomyocyte hypertrophy and increased ECM deposition (Horn & Trafford, 2016). Dysregulation of the ECM at the molecular level leads to fibrosis, which results in whole organ dysfunction due to increased wall stiffness. Accordingly, there has been age-associated left ventricular fibrosis observed in mice (Bradshaw et al., 2010), rats (Sun, Zhang, Zhang, & Lamparter, 2000), dogs (Asif et al., 2000) and humans (Gazoti Debessa et al., 2001; Mewton, Liu, Croisille, Bluemke, & Lima, 2011).

Moreover, hypertrophic cardiomyocytes require higher oxygen and energy levels, creating a more hypoxic environment, and thereby increasing free radical production that damages cellular components. In hypoxic environments with increased ROS, cardiomyocytes release pro-inflammatory cytokines to stimulate an immune response. This causes an increase in macrophage numbers in the myocardium, upregulating the number of MMPs present, particularly MMP-9 (Meschiari et al., 2017). It has also been noted that an increase in MMP levels in aged mice myocardium has been associated with an increase in inflammatory responses, increasing ECM deposition and decreasing angiogenic capacity. This thereby alters the overall

cardiac ECM composition, which could affect remodeling post-MI, particularly in the aged myocardium.

ECM homeostasis is very important for myocardial structure and function since it depends on the balance of synthesis and degradation (Meschiari et al., 2017). One of the main components of the ECM is collagen- with all forms in which their ratio, and protein forms reflect the overall quality of the ECM. Although collagens type I (~85%) and III (~11%) are the most abundant in the myocardium of young adult tissues, with age the ratios of type I and type III are altered (Horn & Trafford, 2016). An increased ratio of type I to III may contribute to LV stiffness (Meschiari et al., 2017), from an increase in ECM cross-linking thereby increasing overall tissue stress. Understanding these age-associated changes in the ECM may lead to new therapeutic targets for improving cardiac repair post-MI in the elderly population.

1.7. Research Plan

1.7.1. Rationale

Aging is associated with the progressive deterioration in structure and function of the heart, likely contributing to the development of CVD, as well as causing complications and poor recovery post-MI. With an increase in the elderly population, it is of importance to understand the changes that occur with aging at the cellular and molecular level that can contribute to the increased risk of CVD, particularly within the ECM environment. Recent evidence suggests an important role for the CCN family of matricellular proteins in modulating cell-matrix interactions and modifying cellular signals involved in the cardiac repair and remodeling process. However, the role of Nov and Wisp1 remains to be better elucidated in aging and post-MI repair. By determining the age-associated effects of matricellular proteins we may gain insight on how to exploit their functions for the development of new treatments for MI.

1.7.2. Aims and Objectives

1. To determine if there is an age-associated change in expression of the matricellular proteins Nov and Wisp1 in the mouse heart.
2. To determine how a change in Nov and Wisp1 expression may be related to repair and remodeling post-MI with particular interest on their function in cardiac fibroblasts.

1.7.3. Hypotheses

- Nov and Wisp1 will be differentially expressed between young and old female mice.
- Their expression post-MI will vary based on their role in the repair and remodeling process, along with the age of the animal.
- Both Nov and Wisp1 will have an effect on cardiac fibroblast function, which may be related to the repair and remodeling of the myocardium post-MI.

Materials and Methods

Materials and Methods

2. Materials and Methods

All animal work was performed in accordance with the National Institute of Health Guide for the Care and Use of Laboratory Animals with the approval of the Animal Care Committee at the University of Ottawa Heart Institute under protocol number HI-2039.

2.1. In Vivo and In Vitro Sample Collection

2.1.1. Experimental MI Mouse Model and Echocardiography

Female 6-8-week-old C57BL/J6 mice and 10-14-month old female C57BL/J6 retired breeding mice (Charles River, Sherbrooke, QC, Canada) arrived at the Heart Institute one week prior to use/procedures to allow for acclimatization. One hour prior to surgery, mice were administered 0.1 mL buprenorphine to minimize pain and discomfort, then anesthetized with gaseous 2.5% isoflurane with 2% oxygen as previously described (Blackburn et al., 2015).

The left anterior descending coronary artery (LAD) was ligated using a 6.0 silk suture (Syneture) with two stitches to produce appropriate blanching 2mm below the top of the left atrium. The rib separator was removed, and skin was closed with #5 synthetic thread (Syneture). At three time-points following LAD ligation: i) 2 days, ii) 7 days, and iii) 14 days, echocardiography (Visualsonics, Vevo770 system) was taken prior to sacrifice to assess cardiac function on the long-axis views, using B mode with the 707B scan head probe. Analysis of echocardiography was performed using the manufacturer's supplied software, manually tracing the systolic and diastolic images. Echocardiography was also taken at the healthy/baseline (no MI) time point as a control.

Cardiac tissue samples were dissected from the infarct/peri-infarct zone, and border zone at each timepoint listed above and either: i) stored in 4% PFA (Paraformaldehyde) at 4^{o}C for 24 hours for cryo-sectioning, ii) stored at -80^{o}C to be homogenized later for RT-qPCR for mRNA expression, or iii) stored at -80^{o}C to be homogenized later for protein expression profiling using Western blot.

All animals under the healthy category did not undergo LAD ligation, however tissues were collected at the same timepoints listed above, in the same manner.

2.1.2. Cardiac Tissue Isolation

Healthy female C57BL/J6 wild type mice and 2, 7 and 14-days post-MI mice (young and old as previously described) were anesthetized with gaseous 2.5% isoflurane with 2% oxygen, followed by cervical dislocation. The bench, mice and tools were sprayed with 70% ethanol to keep the tissue free of bacteria. The chest cavity was opened by cutting diagonally from the bottom of the sternum, through the ribs, to just under the front limbs on both sides. The heart was then cut out from the cavity with small scissors and fat was removed from the tissue. The aorta was removed just enough to see the right and left ventricle areas and the heart was perfused with sterile PBS using a 25G needle attached to a filtered syringe to flush blood out of the chambers. The right ventricle was removed using small scissors and the infarct area and infarct border zone were separated and placed in sterile Eppendorf tubes. The tubes were directly placed in liquid nitrogen for freezing, and these tissues were used for RNA and protein isolation.

For hearts to be used for histology and immunohistochemistry, whole hearts were perfused with sterile PBS and then placed in lmL of 4% PFA at 4^{o}C overnight for fixation in a sterile Eppendorf tube. The following day tissues were washed 3 times with PBS and placed in a

new Eppendorf tube with 1.5mL sucrose (30%) and placed at 4^{o}C for 24-48 hours. Once the heart was completely saturated in sucrose, sinking to the bottom of the tube, they were snap frozen in OCT and stored at -80^{o}C for sectioning. These hearts were sectioned for histology and immunohistochemistry.

2.1.3. Histology and Immunohistochemistry

Slides of heart sections were prepared with 10um sections at different levels of the heart, started at the apex. Sections were obtained using ThermoScientific HM550 Cryostat. Masson's trichrome staining was performed to measure the relative scar size by the midline-arc method as previously described by Takagowa et al. (Takagawa et al., 2009). All primary antibodies for immunohistochemistry were purchased from Abcam: α-SMA (abcam; 5694), active-caspase-3 (abcam; 13847), and the Alexa Fluor (488, 555) secondary anti-rabbit and anti-rat antibodies were from Invitrogen (A11034, A21208). To assess α-SMA positive cells (for activated fibroblasts), sections were stained with Zenon Alexa Fluor 488 reagent IgG1 (1:600) and α-SMA primary antibody (1:250, abcam; 5694). Apoptosis was identified using an anti-active caspase 3 antibody (1:100). Imaging was performed with a Zeiss Z1 fluorescence microscope and ZenBlue (2011-2012) digital image software (20× magnification). For quantification, 3 random microscopic images were obtained from the infarct and 4 from the border zones and counted per sample for an average value in a blinded fashion.

2.1.4. Cardiac Fibroblast Isolation and *In Vitro* Culture

The collection of tissue for fibroblast isolation is very similar to that described in the previous section (2.1.2) except no echocardiography was performed prior to sacrifice. Hearts

were collected from female C57BL/J6 wild type mice at 8-12 weeks of age (no MI). Following the removal of the tissue from the mouse and perfusion with sterile PBS to flush out the blood, the tissue was placed in a sterile Eppendorf tube containing sterile PBS. PBS was then removed, and the tissue was finely minced using small scissors. The minced tissue was placed in 700uL of HBSS and 300uL of digestion buffer (collagenase (Gibco-17101-015) and dispase (Gibco)) and mixed well with vigorous pipetting. The tube was heated for 40 minutes at 37^{o}C until all pieces of the tissue could easily go through the tip of the pipette. The tube was centrifuged at 300g for 5 minutes, and the top aqueous layer was removed from the large pellet. 1mL HBSS was added to wash the cell pellet and spun again. These steps were repeated until a clear aqueous layer could be removed from the pellet. Cells were resuspended in 1mL DMEM F-12 high glucose media (Gibco) containing 10% FBS (Gibco) with 1% pen/strep added. The cell-media mixture was then mixed through pipetting and placed in a 10cm plate and topped up with 10mL total media and placed at 37^{o}C for 4 days. Media was replaced with new media after 24 hours. Once approximately 90% confluent, the cells were lifted using 4mL Trypsin/EDTA (Thermo Fisher; 25200056) in 37^{o}C for 5 minutes. Cells were gently pipetted and collected into a 15mL Falcon tube containing 2-3mL media. Plates were washed with PBS and added to the Falcon tube. The tube was spun at 300g for 5 minutes. Following centrifugation, the supernatant was removed, and the cell pellet was resuspended in 1mL media. 10uL was removed and added to a hemocytometer to manually count the cells. All cells were seeded tissue culture polystyrene plates (TCPS) at a density of 1.0×10^{6} cells for 6-well plates, 0.4×10^{6} cells for 12-well plates and 0.2×10^{6} cells for 24-well plates.

2.1.5. Cardiac Fibroblast Culture Conditions and Treatments

All *in vitro* cell culture was performed in regular growth culture conditions in a sterile incubator (Thermo Scientific) (37^{o}C, 5% O_2) unless otherwise stated. Hypoxic conditions were performed at 37^{o}C, with 1% O_2. Once lifted and seeded, all cells were left for 3-4 hours to adhere to the plate prior to treatment. Cardiac fibroblasts were treated with 0.2ug/mL Mouse Transforming Growth Factor β1 (TGF-β1 (neb; 5231LC)) where stated and 10% total media volume with either Nov conditioned Hek293 media (0.0095ug/uL) or Wisp conditioned Hek293 media (0.014ug/uL) and non-transfected, conditioned Hek293 media as a protein control (0.0093ug/uL). These treatments were used for the Ki67 proliferation assay, viability assay and to analyze mRNA and protein expression of various targets.

2.1.6. Macrophage Culture Conditions

Macrophages were isolated from bone marrow derived macrophage (BMDM) cultures after 7 days of culture as described by Blackburn et al. (Blackburn et al., 2015). Cells were lifted, counted and resuspended as previously explained and re-plated on 6-well plates at a density of 4.0×10^{6} cells in 2mL. Cells were cultured as M0 macrophages using DMEM media (Gibco) with 10% FBS and 15% L929 media (Cancer cell line) or polarized to M1 macrophages using 2uL of 1ug/mL lipopolysaccharide (LPS; Sigma-L4391-1MG) and 2uL of 100ng/mL interferon gamma (IFNy; R&D Systems), or to M2 macrophages using 2uL of 10ng/mL interleukin-4 (IL-4; Peprotech-214-14), and then incubated at 37^{o}C for 3 days. Cells were then treated with TRIzol for RNA isolation.

2.2. RNA Isolation

2.2.1. Cardiac Tissue RNA Isolation

To avoid any sample being contaminated with RNases, the lab bench and mortar and pestles were sprayed with RNase Away (Thermo Scientific). Tissues frozen in liquid nitrogen were placed in sterile mortar and pestles that were chilled at -80^{o}C. Tissues were crushed in the mortars and pestles and 100 mg was added to a clean 1.5 mL Eppendorf tube. 1 mL of TRIzol/TRI-Reagent (Zymo Research) was added to the crushed cardiac tissue and pipetted vigorously for homogenization. Following 10 minutes at room temperature, 0.2 mL of chloroform was added, shaken intensely for 30 seconds and left to separate for 15 minutes at room temperature. The tubes were spun at 12000g for 15 minutes and the top phase containing RNA was then transferred to a clean 1.5mL tube for washing and precipitation with 0.5mL isopropanol. The aqueous mixture was then left at -20^{o}C to precipitate for 1 hour. The tube was then spun at 12000g for 10 minutes, aspirating the clear supernatant from the RNA pellet. 0.5mL of ice-cold 75% ethanol was added to wash the pellet, inverted and spun at 7500g for 5 minutes. The clear ethanol layer was removed, and the excess liquid was set to air dry for 10 minutes at room temperature. 30uL of RNase free water (Invitrogen) was added to the tube and heated at 40^{o}C for 5 minutes to dissolve the RNA.

2.2.2. Cultured Cell RNA Isolation

To isolate RNA from cultured cells a similar procedure to that described above for cardiac tissue RNA isolation was used. TRIzol was added directly to the well, placed on a shaker for 5 minutes and pipetted up and down to transfer to a clean 1.5mL Eppendorf tube. The RNA pellet was allowed to air dry and reconstituted in 15-20uL RNase free water (Invitrogen).

2.2.3. RNA Quantity and Quality

All RNA was analyzed using the NanoDrop-1000 Spectrophotometer with V3.3 Software (Thermo Scientific). The machine was blanked with 1uL of RNase free water (Invitrogen) and tested with the same RNase free water sample prior to analyzing the RNA sample of interest. 1uL of the sample was added to the analyzing platform, and analyzed with the arm closed, displaying the RNA concentration in ng/uL, 260/280 (protein contamination measure). All samples used had 260/280 ≥ 1.9. If an RNA sample had a low or high 260/280 value, samples were cleaned up with a DNase purification technique: 0.5uL DNase, 41uL RNase free H_2O, 9uL DNase buffer (Invitrogen). This mixture was heated for 10 minutes at 37^{o}C, following addition of 0.2M EDTA (pH 8.0), with heat applied for 10 minutes at 75^{o}C to precipitate RNA transcripts. These consistent values ensured PCR data was reliable.

2.3. Quantification of Matricellular Proteins and Other Targets

2.3.1. Reverse Transcription and qPCR for Matricellular Protein Targets

Primers for the matricellular proteins Nov and Wisp1 were identified and ordered (IDT DNA) for the study of gene expression after searches on NCBI and Primer3. All other primers were previously designed in the lab and tested for efficiency prior to use, spanning at least two exons in length. The following primers were used:

Common Name	Gene Abbreviation	Primer Direction	Sequence
Nephroblastoma overexpressed	Nov	Forward	GCCTATAGACCGGAAGCCAC
		Reverse	CTTGTTCACAAGGCCGAACG
Wnt-inducible signaling protein 1	Wisp1	Forward	GTGCTGTAAGATGTGCGCTCA
		Reverse	CACTCCTATTGCGTACCTCGG
Housekeeping	18S	Forward	AAACGGCTACCACATCCAAG
		Reverse	CCTCCAATGGATCCTCGTTA

Housekeeping	Beta-actin	Forward	TGGGAATGGGTCAGAAGGAC
		Reverse	TGAAGCTGTAGCCACGCTCG
Alpha-smooth muscle actin	a-SMA	Forward	GTCCCAGACATCAGGGAGTAA
		Reverse	TCGGATACTTCAGCGTCAGGA
Tenacin-C	TnC	Forward	GAGCCCCTTTGCCTCAACAA
		Reverse	CTTCGCCCGTGAAACCTTCTT
Thrombospondin-1	TSP1	Forward	CCTGCCAGGGAAGCAACAA
		Reverse	ACAGTCTATGTAGAGTTGAGCCC

Table 1. List of Genes and Primers used for RT-qPCR Analysis.

RNA isolated was transcribed to cDNA using SMARTScribe Reverse Transcription (TaKaRa). A master mix containing 0.5uL of 20uM Random Hexamers (Invitrogen), 1uL of 10mM dNTP Mix (GeneDirex), 5uL H_2O was added to a tube containing 4.5uL of RNA (2ug of total RNA). The RNA mixture was loaded into the MYCycler (BioRad) and ran with the program: 72^{o}C for 3mins, 4^{o}C for 30sec, followed by 20^{o}C for 10mins, where in the last 1 minute a solution containing 2uL 5× First-Strand Buffer (TaKaRa), 1uL DTT (TaKaRa) and 0.5uLSMARTScribe Reverse Transcriptase was added. The program continued with: 42^{o}C for 60mins, 75^{o}C for 15mins, finishing with 4^{o}C for 30mins and stored at -20^{o}C.

To complete the RT-qPCR, a master mix for each gene of interest was prepared in duplicate to accommodate loading on the plate. The volumes of each of the ingredients in the reaction are: 10uL 2× SensiFAST SYBR No-ROX Mix (Bioline), 0.8uL of 10uM forward and reverse primers combined, 6.2uL ddH_2O, 0.5uL iCycler iQ External Well Factor Solution (BioRad) and 1uL of cDNA. Plates were loaded with 20uL in each PCR strip of tubes and placed in the iCycler (BioRad) and programmed to complete the following: 40^{o}C for 30sec, 95^{o}C for 2 mins for activation followed by repeating 45 cycles of denaturation for 20sec at 60^{o}C, then 20sec at 72^{o}C, and annealing/extension for 30sec at 55^{o}C, 95^{o}C for 30sec, 60^{o}C for 1min, followed by a

melting curve step. Relative quantification was used with gene expression normalized to housekeeping gene expression.

2.3.2. Protein Isolation and Western Blots

Protein was isolated from frozen tissues as mentioned previously and crushed using sterile mortar and pestles. 1mL of RIPA buffer (1M Tris HCl, pH 6.8, 5M NaCl, 1% SDS, 97% sodium deoxycholate, Triton-X 100, ddH_2O and protease inhibitor pellet (Roche)) was added per 100mg of ground tissue, pipetted intensely for homogenization and shaken on high at 4^oC for 2 hours. The same technique was used for cultured cells with 1mL RIPA buffer added per well (12-well plate). The protein concentrations were calculated using the Pierce BSA Protein Assay Kit (Thermo Scientific), using BSA standards following the manufacturer's instructions. 20ug protein was added per well in the Western gel.

The separating gel was made using 6.9mL ddH_2O, 4.8mL of 40% acrylamide, 4mL of 1.5M Tris HCl (pH 8.8), 160uL of 10% sodium dodecyl sulfate (SDS), 160uL of 10% ammonium persulfate (APS) and 16uL of tetraacetylethylenediamine (TEMED) in a 50mL Falcon tube and filling the gel plate to 1cm from the top. A thin layer of isopropanol was added to the top and left to solidify for about 1 hour. The stacking gel containing 5.8mL ddH_2O, 1.5mL of 40% acrylamide, 2.5mL of 0.5M Tris HCl (pH 6.8), 100uL of 10% SDS, 100uL of 10% APS and 10uL TEMED was then added on top of the separating gel, with a 15-well comb inserted. Once solidified, the gels were wrapped in moist paper towel and placed at 4^oC overnight. Samples were prepared by adding 5× Loading buffer (Laemmli buffer: 3.55mL ddH_2O, 1.25mL 0.5M Tris HCl, pH 6.8, 2.5mL glycerol, 2mL 10% SDS, 0.2mL 0.5% Bromophenol blue) for electrophoresis by boiling at 95^oC for 10 minutes, then loaded to the 12% sodium dodecyl

sulfate-polyacrylamide gel electrophoresis (SDS-PAGE) gel with 1 well containing 5uL EZ-RUN Pre-Stained Rec Protein Ladder (Fisher BioReagents). Once loaded, the chamber was filled with Running buffer (25mM Tris Base, 192mM glycine and 3.5mM SDS with ddH_2O) and ran at 120V for approximately 90 minutes. Once the dye-front reached the bottom of the gel, the running was stopped, and the gel containing proteins was transferred to a nitrocellulose membrane for 90 minutes at 100V, in a chilled chamber containing 100mL of 10× transfer buffer (25mM Tris Base and 192mM Glycine) with 200mL methanol, and 700mL ddH_2O.

Following transfer, membranes were cut and stained with Ponceau S to ensure bands were present prior to blocking in 5% w/v dry milk in TBST (100mL of 10× TBS (50mM Tris Base and 150mM NaCl with H_2O, pH 7.4 (adjusted with HCl)), 900mL ddH_2O and 1mL Tween-20 (Sigma)) for 1 hour at room temperature on a plate shaker (Scilogex). Primary antibodies were added to the blots, diluted in blocking solution: CCN3/Nov (1:1000; Cell Signaling Technologies; 8767S), Wisp1 (1:1000; abcam; 178547), α-SMA (1:1000, abcam; 5694) and loading control, β-actin (1:5000; abcam; 8227) and incubated overnight at 4^oC. Primary antibodies were then removed, and the blots were washed 3× with TBST for 10 minutes before the secondary antibodies were added, 1:10000 dilution of anti-Rabbit IgG Secondary HRP-linked (Novus) and 1:1000 anti-Mouse IgG, HRP-Linked (Cell Signaling Technologies). After 1 hour of shaking at room temperature, the antibody was removed, and the blots were washed 3× with TBST for 10 minutes before incubation with equal volumes of Novex ECL HRP Chemiluminescent Substrate Reagent Kit (AP Chemiluminescent Substrate and AP Chemiluminescent Substrate Enhancer (20×)) for 5 minutes in the dark. The blots were then developed using CL-XPosure Film (Thermo Scientific), scanned and analyzed on ImageJ using pixel quantification of protein bands, normalized to β-actin loading control.

2.5. *In Vitro* Functional Studies

2.5.1. Preparing Recombinant Nov and Wisp1

DH5α competent cells (Thermo Fisher Scientific) were aliquoted into sterile 1.5mL Eppendorf tubes for a volume of 50uL to start the DNA transformation. 1uL of Nov plasmid DNA (Origene; MR205398; 0.1ug/uL) or Wisp1 plasmid DNA (Origene; MC202062; 0.1ug/uL) was added to the cells, flicking to mix. The mixture was then placed on ice for 15minutes, followed by heat shock for 45 seconds at 42^{o}C. 200uL of sterile SOC microbial growth media (LB Broth (Invitrogen), ddH_2O and 1M glucose) was added to the tube and shaken vigorously for 1 hour at 37^{o}C. LB Plates were made using LB Broth (Invitrogen), agar (Invitrogen) and antibiotic solution Ampicillin (Sigma). Aliquots of the DH5α cell culture were spread on the LB plates to allow for colony growth overnight at 37^{o}C. Colonies grown that were specific to the plasmid DNA inserted were isolated and incubated overnight in 3-5mL of SOC media, containing the Ampicillin antibiotic specific to the plasmid DNA insert. The cultures were spun down, and the DNA was isolated using Zyppy Plasmid Miniprep Kit (Zymo Research) and GenElute HP Plasmid Maxiprep Kit (Sigma) according to manufacturer's instructions. DNA integrity and concentration were determined using the Nanodrop as previously described for determining RNA concentration. The DNA was digested using BamHI and Not1 (Fermentas) at 37^{o}C for 1 hour: (2uL Buffer O, 1uL BamHI, 0.5uL NotI, 15.5uL H_2O and 1uL DNA. A 1% LE agarose gel was made (Invitrogen), loaded and ran with 1× TAE buffer (Tris Base, Acetic acid and EFTA). Each digested plasmid DNA sample was run with their representative DNA plasmid construct as a positive control, with 2uL loading buffer. The gel was run at 100V for 1 hour and visualized on the BioDoc-it imaging system (BioRad) to identify that the transformation was successful. Images for the transformation can be visualized in Appendix A.

The isolated DNA was then used for Hek293 cell transfection. Hek293 cells were cultured, split and reseeded in the same method as described previously for the culture and splitting of fibroblasts. The night prior to the transfection, the media was changed to remove Penstrep (Invitrogen) antibiotics and the following morning, the transfection took place with Lipofectamine 3000 (Invitrogen), and 0.5uL DNA per well as described on the manufacturer's protocol. The cells were cultured in the presence of the plasmid DNA at 37^{o}C, with a media change after 24 hours to remove any excess DNA. For the next 3 consecutive days, the media was collected and spun down in 1mL aliquots at 1000g for 5mins. GFP-plasmid was used to ensure the Lipofectamine 3000 protocol was successful and imaged on the microscope previously mentioned. The media was analyzed using Western blot as described previously, running the gel with recombinant Mouse CCN3 protein/Nov (Novus; NBP2-35100; 0.5mg/mL) and Human Wisp-1 protein (Pepro Tech; 120-10-5UG; 0.5mg/mL) on a known concentration to determine the concentration of the Hek293 media collected. This was used as a cell treatment for the assays described in the sections below (2.5.2, 2.5.3). Hek293 conditioned media, without DNA transfection, was used as a total protein control for *in vitro* experimentation.

2.5.2. Fibroblast Proliferation Assay

Cardiac fibroblasts were cultured as described previously and seeded onto the slide of a chamber slide system with a detachable well (Fisher) and left to adhere. Cells were treated with sterile; i) TGF-β, ii) TGF-β and 10% Nov, iii) TGF-β and 10% Wisp1, iv) 10% Nov, v) 10% Wisp1, vi) non-transfected Hek293 media, and vii) no treatment. After 48 hours of culture at 37^{o}C, the media was removed from the wells and 300uL of ice cold 4% PFA was added to fix the cells. Each well was washed 3× with PBS before antigen retrieval. A sodium citrate solution (pH

6.0) containing the slides was brought to a boil for 4-5 minutes and left to cool to room temperature. The slides were removed from the solution and placed in PBS with 0.2% Triton-X for 10 minutes prior to blocking with 10% FBS in PBS for 1 hour. Following the blocking step, cells were stained with primary antibody for Ki67 (1:500 with blocking solution; abcam) at room temperature for 2 hours. Each slide was washed 3× with PBS for 5 minutes and the secondary antibody Zenon Alexa Fluor 488 IgG1 (1:600 in PBS; Life Technologies) was added and incubated in the dark at room temperature for 1 hour, followed by 3× PBS washes. A small amount of ProLong Gold antifade reagent with DAPI (Invitrogen; 15uL) was added to the slide, with a cover slip and imaged with the Zeiss Z1 fluorescence microscope and ZenBlue (2011-2012) digital image software (5× magnification). For quantification, 5 random microscopic images were obtained from each slide and the number of proliferating (Ki67+) cells was quantified and compared to the total cell number (DAPI+).

2.5.3. Fibroblast Viability Assay

Cardiac fibroblasts were cultured and seeded as previously described in a sterile 12-well plate. Cells were let to adhere for 3 hours in regular culture conditions prior to treatment with: i) TGF-β (0.2 ug/mL); ii) TGF-β (0.2 ug/mL) and 10% Nov media; iii) TGF-β (0.2 ug/mL) and 10% Wisp1 media; iv) 10% Nov media; v) 10% Wisp1 media; vi) non-transfected Hek293 media; or vii) no treatment. Cells were cultured for 48 hours in hypoxic conditions (37^{o}C, 1% O_2). Viability was assessed by adding 300uL of Live/Dead Viability/Cytotoxicity Kit (Life Technologies; L3224) reagent mixture (1:2000 Calcein, 1:500 Ethidium homodimer) to each well, and incubating in the dark for 30 minutes at 37^{o}C. Three images of each well were taken at random using the Zeiss Z1 fluorescence microscope and ZenBlue (2011-2012) digital image

software. Images were quantified using ImageJ and the percentage of viable cells was quantified, taking the average of each well. This was in a blinded fashion (10× magnification).

2.6. Statistical Analysis

Values are presented as a mean ±standard error (SE). For RT-qPCR and Western blot, data was reported as the mean fold-change of treatment to control group. All data was analyzed with a two-tailed t-test or ANOVA using GraphPad Prism 7 software unless otherwise specified. Probability values of $P<0.05$ were considered statistically significant.

Results

Results

3. Results

3.1. Identifying Differences in Healthy and Post-MI Young vs Old Mice

3.1.1. LVEF is Reduced in Old Mice at 14 Days Post-MI Compared to Young Mice

It has been shown that elderly patients, women in particular, have a higher incidence of fibrosis and hypertrophy of the left ventricle (LV), predisposing them to heart failure with reduced ejection fraction after an ischemic event (Paneni et al., 2017). Therefore, to assess whether there is a difference in cardiac function post-MI in young vs old female mice, we performed echocardiography at baseline (no MI), and following a LAD ligation at 2 days, 7 days and 14 days post-MI. The left ventricular ejection fraction (LVEF) was measured using echocardiography to assess cardiac function. As shown in figure 3A, we found that at 14 days post-MI there was a reduction in LVEF in old animals compared to young, with no difference detected at 2, or 7 days post-MI. We looked to further explore cardiac function and remodeling post-MI by assessing collagen-based scar size to see if there is an increase in old, compared to young since aged hearts are more likely to have an increase in collagen deposition and cross-linking (Meschiari et al., 2017). Although there was a decrease in cardiac function at 14 days post-MI (%LVEF), the Masson's Trichrome staining for scar formation was no different in old compared to young at 14 days (Fig. 3B and 3C). Therefore, it appears that at 14 days post-MI, there is a reduction in cardiac function in terms of LVEF in old animals compared to young, yet, the infarct scar size not different between the two groups.

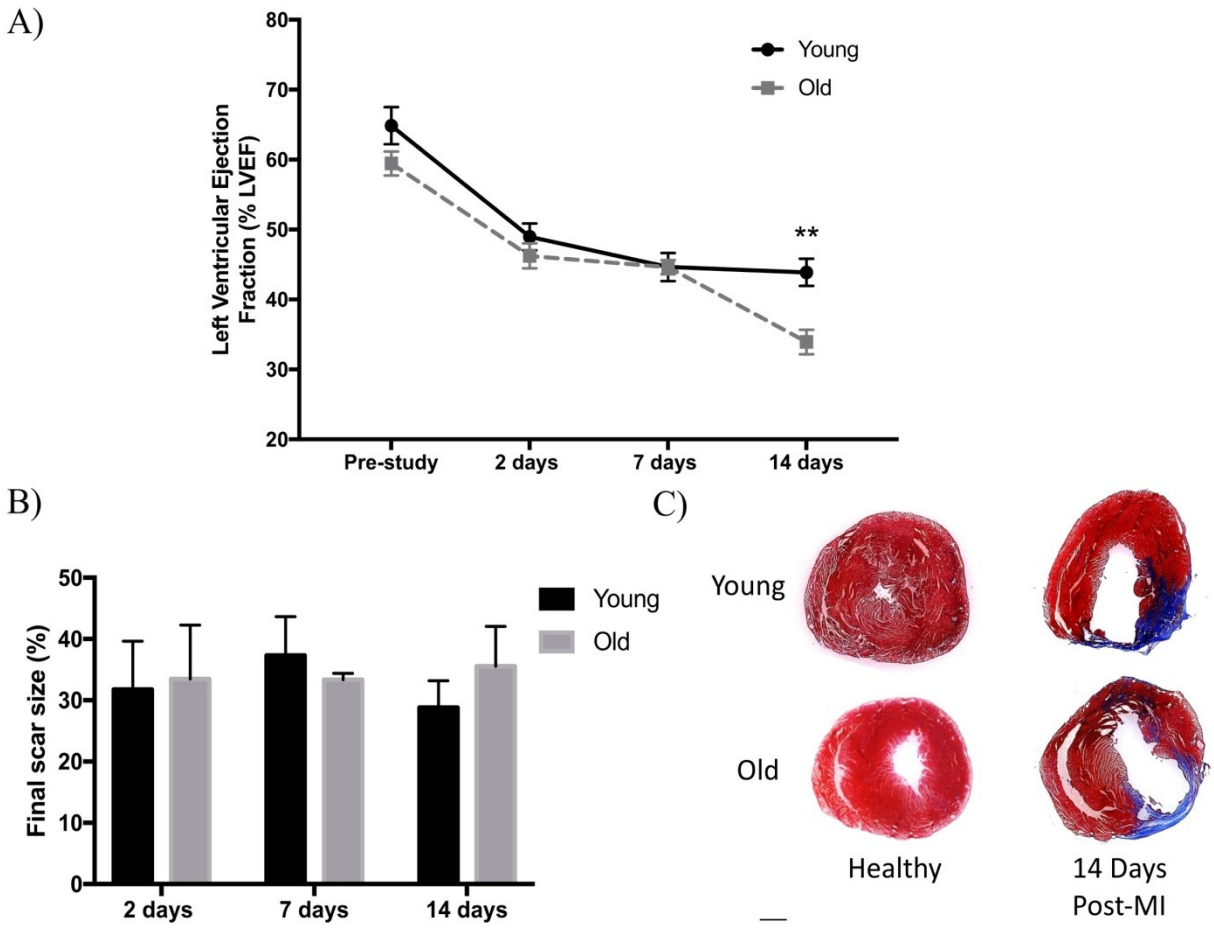

Figure 3. Cardiac Function Assessment in Female Old vs. Young Mice Post-MI. **A)** Ejection fraction (%LVEF) in young (6-8 weeks) (n=7) and old (10-14 months) (n=11) mice showing significantly reduced LVEF at 14 days post-MI in old mice (***p=0.*002). **B)** Final scar size was assessed at 14 days post-MI using midline method, showing no difference between young and old mice (scale bar = 1mm). **C)** Representative images of Masson-Trichrome stained tissue sections, blue representing scar formation and red representing healthy tissue. Data are presented as mean ± SEM.

3.1.2. mRNA Levels of Matricellular Proteins in Healthy and Post-MI Tissues have Altered Expression

Since we established that young and old female mice respond differently post-MI in terms of cardiac function (LVEF), our next goal was to identify if there was a change in the expression of matricellular proteins in the healthy myocardium in young versus old animals. Specifically, we evaluated members of the CCN family of matricellular proteins: Nov and

Wisp1, tenacin (TnC) and the thrombospondin (TSP-1) family. Notably, there was a significant reduction in Nov, Wisp1, TnC and TSP-1 mRNA observed in the myocardium of old mice compared to young (Fig. 4A). This is a potential indication of a reduced function of matricellular proteins in the myocardium with age.

Based on these results, we next decided to focus on two particular members of the CCN family of matricellular proteins: Nov and Wisp1. Nov and Wisp1 were chosen for additional study because of the evidence in the literature for their possible role in angiogenesis, fibrosis and ECM remodeling (Borkham-kamphorst et al., 2012; Dobaczewski et al., 2011; Marchal et al., 2015; Tao et al., 2016; Venkatachalam et al., 2009)(Franogogiannis, 2011). The expression of Nov and Wisp1 were evaluated in the scar and border zone of post-MI hearts of young versus aged mice over a period of 2 weeks. RT-qPCR revealed that post-MI, Nov mRNA is significantly lower in old female mice, compared to young at 2, 7, and 14 days post-MI in the infarct area and at 2, and 14 days post-MI in the border zone (Fig. 4B). Although Wisp1 mRNA expression wasn't significantly different in young compared to old animals at any time point, it follows a similar trend with up to a 17-fold reduction of mRNA levels in old animals compared to young (Fig. 4B).

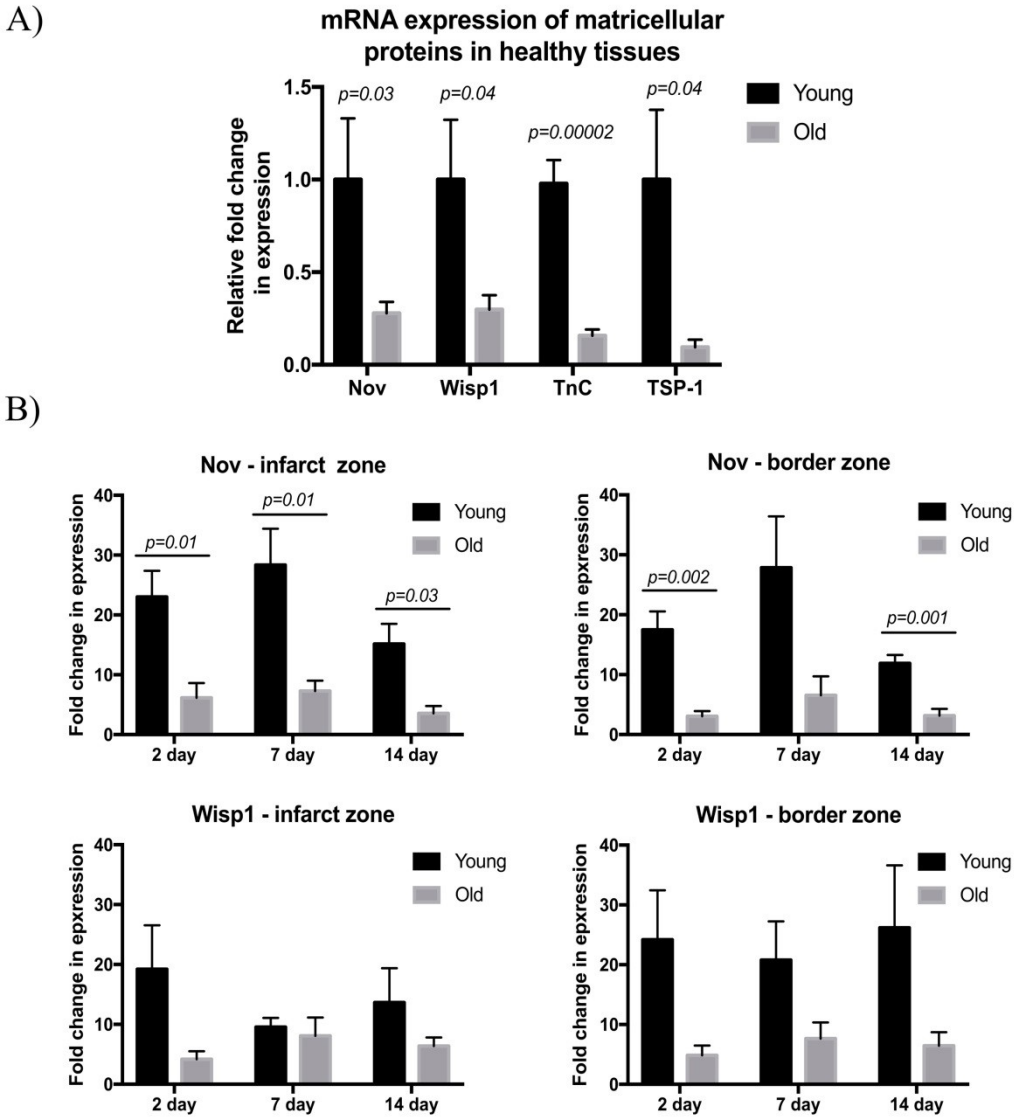

Figure 4. Analysis of Matricellular Proteins mRNA in Healthy and Post-MI Tissues. RT-qPCR analysis of young (n=5) and old (n=5) mouse heart tissue normalized to 18S and β-actin. **A)** Baseline/healthy tissues reveal a 2.5- to 5- fold significant decrease in expression of various matricellular proteins in old tissues relative to young. **B)** Both Nov and Wisp1 show a higher mRNA expression level in young tissues post-MI compared to old tissues post-MI at different timepoints, with only Nov showing significance at 2, 7, or 14 days post-MI.

3.1.3. Protein Levels of Matricellular Proteins in Healthy and Post-MI Tissues Have Altered Expression

The next goal was to identify if the protein expression level of Nov and Wisp1 is altered post-MI in the infarct and border zones. Following LAD ligation and tissue isolation, Western

blot analysis of protein expression levels post-MI was assessed and compared to healthy, non-infarct tissues and normalized to β-actin. It was found that there is a decrease in protein expression level in post-MI tissues at all timepoints compared to healthy myocardial tissue. However, in old animals, there is a larger reduction in protein levels compared to young (Fig. 5). Specifically, Nov expression at 2 days post-MI was significantly reduced in both the border and infarct zone of the myocardium in old versus young mice (Fig. 5A, B). Results also revealed a significant decrease of Wisp1 at 2 and 14 days in the infarct zone (Fig. 5A), and at 7 days post-MI in the border zone (Fig. 5B) of old animals compared to young.

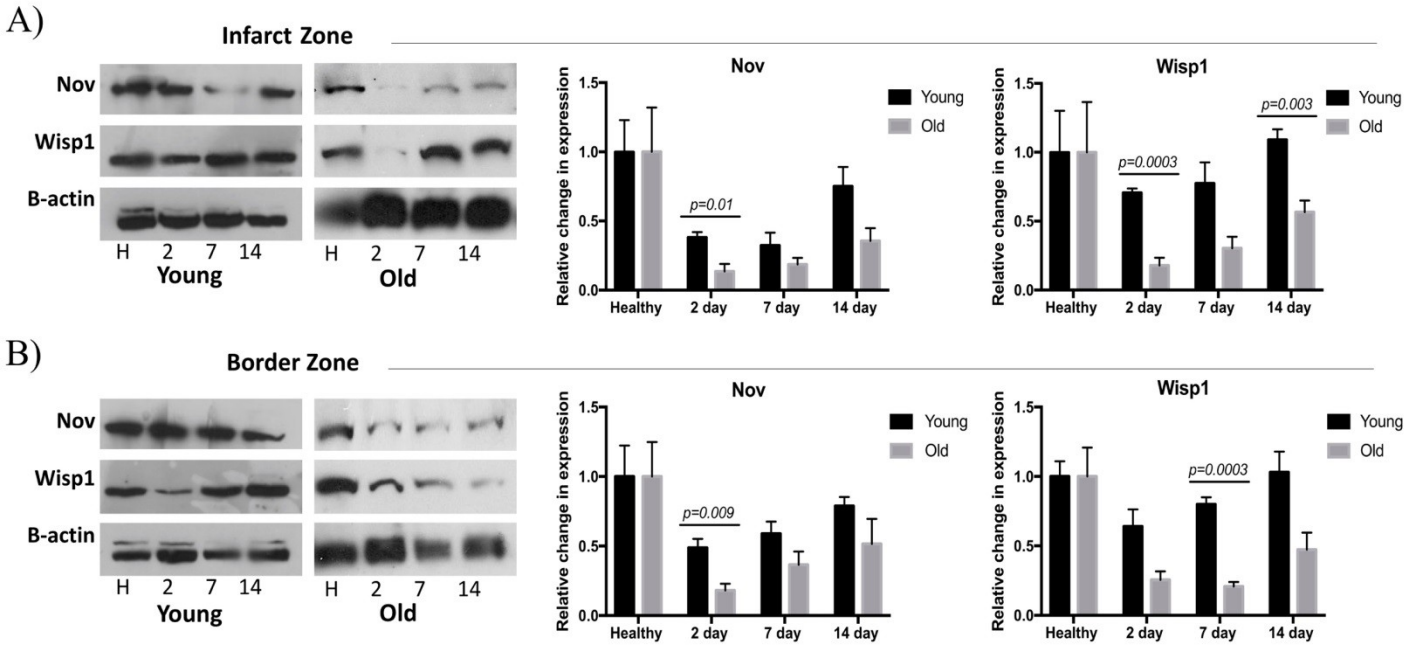

Figure 5. Analysis of Nov and Wisp1 Protein Levels in Post-MI Tissues. Western blot analysis was performed on young (n=4) and old (n=4) mouse heart tissue, and results were normalized to β-actin, and compared to healthy (H), non-infarcted animals. **(A)** In the infarct zone, Nov and Wisp1 show significantly reduced protein levels at 2 days post-MI in old compared to young, as well as Wisp1 at 14 days. **(B)** In the border zone, Nov protein level is significantly reduced in old mice compared to young at 2 days post-MI and Wisp1 at 7 days post-MI.

3.2. Pinpointing a Potential Source of Nov and Wisp1

3.2.1. Cardiac Fibroblasts may be a Potential Source of Nov and Wisp1

As cardiac fibroblasts constitute the largest portion of cells in the myocardium in terms of numbers and are the primary cell type functioning to regulate ECM homeostasis (Chistiakov et al., 2016), we sought to assess if they may be a producer of the matricellular proteins Nov and Wisp1 upon activation. We first treated cardiac fibroblasts for 48 hours with TGF-β to stimulate their activation/transdifferentiation into myofibroblasts, expressing α-SMA. Using Western blot, we were able to confirm the activation of the fibroblasts to myofibroblasts based on the observed increase in α-SMA protein levels (Fig. 6A). Protein levels of Nov and Wisp1 were then analyzed to see their expression after 48 hours of activation *in vitro*. Nov protein levels were significantly increased within the cells upon fibroblast activation (Fig. 6B) and although Wisp1 protein levels showed a similar trend, there was no significant increase (Fig. 6C). This indicates that activated cardiac fibroblasts may produce matricellular protein Nov in the setting of MI.

Since a trend was observed with increased protein expression of Nov and Wisp1 under regular culture conditions, we next looked at the relative mRNA expression levels of Nov and Wisp1 in cardiac fibroblasts under hypoxic conditions. Following culture of fibroblasts under regular growth conditions, cells were treated with TGF-β and exposed to a hypoxic environment (1% O_2, with serum deprivation) thus mimicking the MI environment *in vitro*. After 48 hours of culture, an increase in mRNA expression of α-SMA and Wisp1 was observed with hypoxia and TGF-β stimulation, while no significant difference was observed for mRNA levels of Nov (Fig. 7A, B). Taken together, the RT-qPCR and Western blot data of *in vitro* cardiac fibroblast cultures reveal that Nov and Wisp1 may be produced by activated myofibroblasts in the post-MI myocardium.

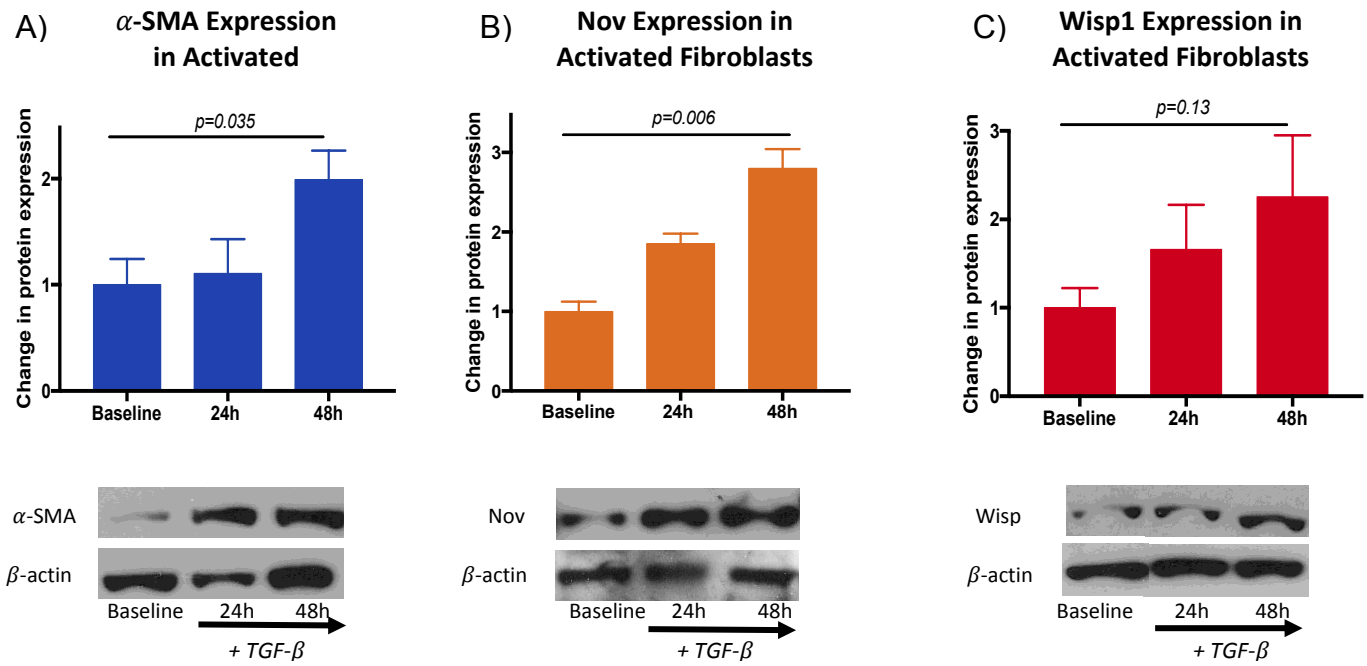

Figure 6. Activated Myofibroblasts Produce the Matricellular Proteins Nov. Protein levels were assessed using Western Blot analysis in an *in vitro* time course study of cardiac fibroblasts cultured with TGF-β for 24 and 48 hours, normalized to β-actin (n=4). **A)** Representative blots showing that TGF-β treatment stimulates α-SMA expression in cardiac fibroblasts after 48 hours. **B)** Nov protein expression was significantly increased in cardiac fibroblasts 48 hours after treatment with TGF- β; however, **C)** only a trend for increased Wisp1 was observed.

Another potential producer of matricellular proteins and cell type of interest was the macrophage, which plays a key role in the inflammatory and proliferation phases of MI. BMDMs were cultured for 7 days and then polarized to either an M1 (pro-inflammatory phenotype), M2 (anti-inflammatory phenotype) or left in the M0 state (undifferentiated phenotype). Cells were treated for 3 days and the mRNA expression levels of Nov and Wisp1 were determined using RT-qPCR. The results revealed a relative increase in both Nov and Wisp1 mRNA expression levels (Fig. 8). Although not significant, the trend suggests that macrophages may be capable of producing these matricellular proteins.

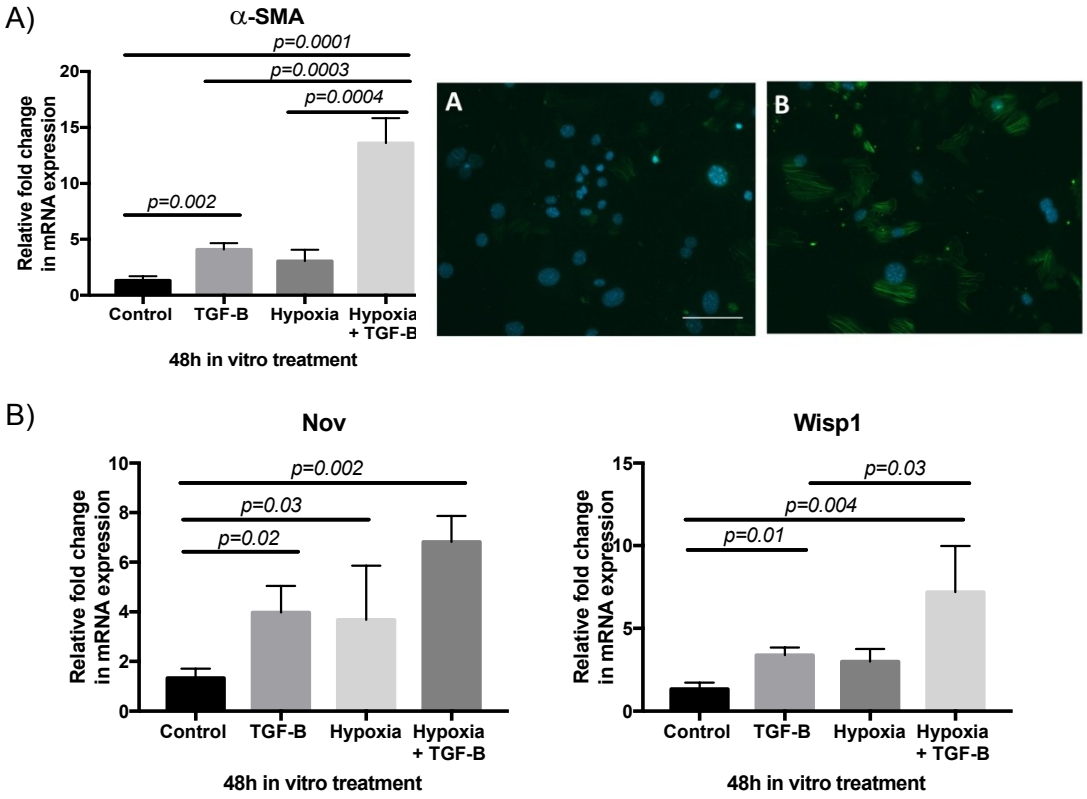

Figure 7. Activated Cardiac Fibroblasts in a Hypoxic Environment Have Increased mRNA Expression of Wisp1. Using RT-qPCR analysis and compared to 18S, mRNA expression levels were assessed in cardiac fibroblasts following 48 hours in hypoxia (1% O2) and treatment with TGF-β (0.2 ug/mL). **A)** α-SMA mRNA expression was significantly increased in fibroblasts cultured under hypoxia and treated with TGF-β treated, indicating myofibroblast activation. On the right are representative immunohistochemistry images of α-SMA stained fibroblasts under control culture conditions or with hypoxia (1% O_2) and TGF- β treatment (Blue = DAPI-staining nuclei and green = α-SMA staining (Scale bar = 50um). **C)** Relative expression of Nov and Wisp1 showing a significant increase in Wisp1 mRNA levels after 48 hours.

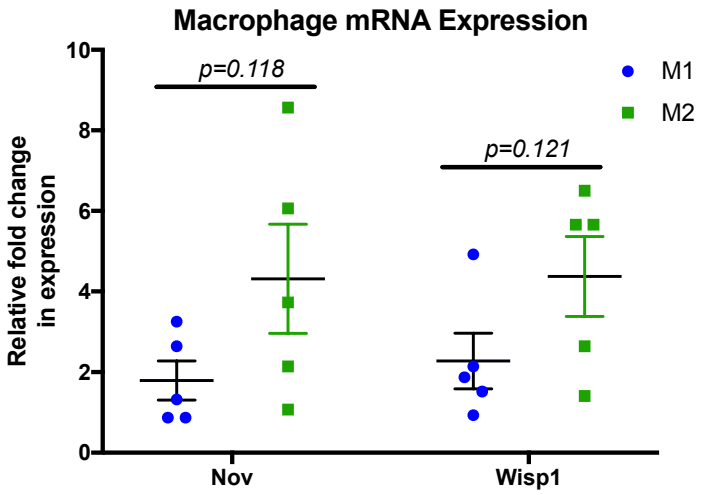

Figure 8. Relative mRNA Expression of Nov and Wisp1 in Activated Macrophages. Macrophages (n=5) were activated with INF-gamma and IPS to an M1 phenotype, or with IL4 to an M2 phenotype, and compared to M0 (undifferentiated macrophages). Using RT-qPCR, results show only a trend for increased expression of Nov or Wisp1 mRNA levels upon macrophage activation to either the M1 or M2 phenotype.

3.3. The Exogenous Cellular Effects of Nov and Wisp1 *in Vitro*

3.3.1. Fibroblast Proliferation is Increased *in Vitro* with Nov and Wisp1 Treatment

Matricellular proteins have many tissue and cell-type specific functions. Since cardiac fibroblast proliferation plays an important role in cardiac repair and remodeling, we wanted to look at the exogenous effects of Nov or Wisp1 on cardiac fibroblast proliferation *in vitro*. Nov and Wisp1 protein for use in these experiments was generated through a transfection procedure using Hek293 cells (Appendix A Fig. 1, 2). The media from transfected cells was collected and used to treat cardiac fibroblasts for 48 hours, after which proliferation was assessed by Ki67 staining. The results demonstrated that in the combination of TGF-β + Wisp1, as well as TGF-β + Nov there was significantly increased proliferation (Fig. 9A, B).

3.3.2. Nov and Wisp1 Pro-Survival Functions on Cardiac Fibroblasts

The effect of Nov and Wisp1 on cardiac fibroblast viability was also assessed *in vitro* under hypoxic conditions to mimic the MI environment (serum deprivation and 1% O_2). Our results showed that there was no difference in total cell number between treatment groups (Fig. 10); however, in the presence (Fig. 10A) and absence of TGF-β (Fig. 10B) there was an increase in the number of viable cells with treatment of Nov or Wisp1. This suggests a potential pro-survival function for Nov and Wisp1 on fibroblasts in the myocardium.

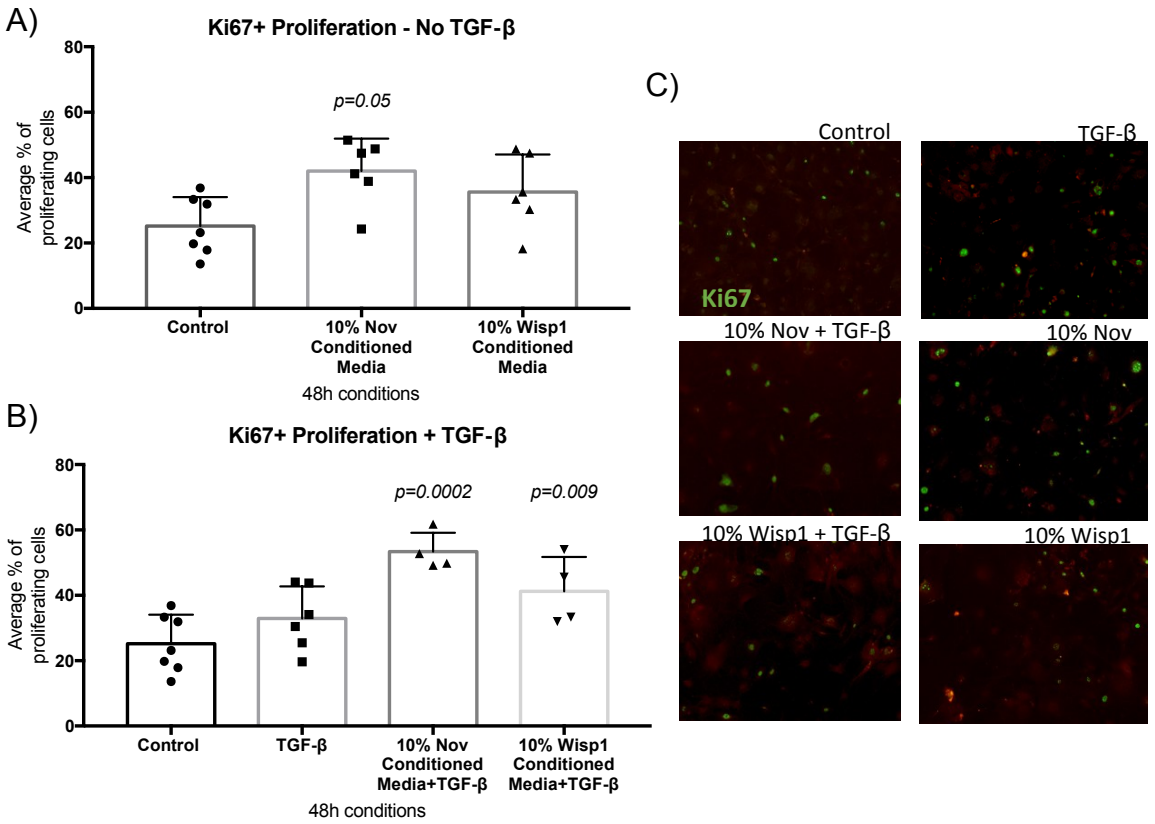

Figure 9. *In Vitro* Fibroblast Proliferation Assay Using Ki67 with Fluorescence Microscopy. **A)** After 48 hours without TGF-β stimulation, cells treated with 10% Nov conditioned media had a significant increase in number of proliferating cells. **B)** In TGF-β conditions after 48 hours, cells treated with 10% Nov conditioned media and 10% Wisp1 conditioned media had a significant increase in proliferation compared to control, un-treated conditions. **C)** Representative immunofluorescence images for fibroblast cultures stained for the proliferation marker Ki67 (green) (Scale bar = 100um).

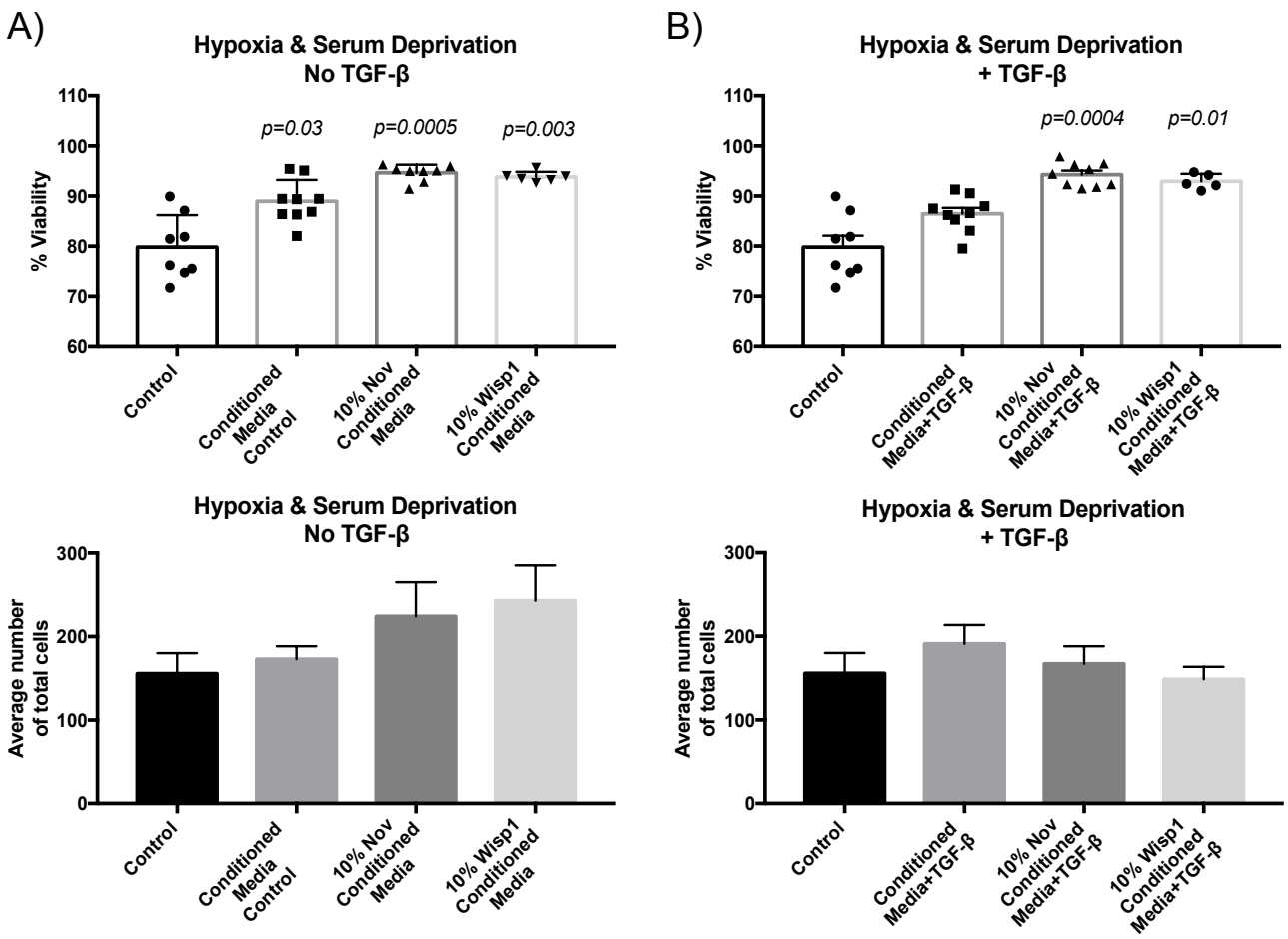

Figure 10. Live/Dead Assay for Cardiac Fibroblasts in Hypoxia and Serum Deprivation for 48 hours. Cells were treated with or without TGF-β (0.2 ug/mL). Using a Live/Dead assay kit and fluorescence microscopy, the viability of cells was determined. **A)** Without TGF-β (n=6), total cell number was not different between treatment groups (lower), while viability was increased when cells were treated with Hek293 conditioned media, Nov conditioned media, and Wisp1 conditioned media, compared to control. **B)** Fibroblasts (n=6) had increased viability under hypoxia and serum deprivation when treated with TGF-β + Nov conditioned media or TGF-β + Wisp1 conditioned media. There was no difference in total cell number between conditions.

3.4. Myofibroblast Numbers in the Infarcted Myocardium

3.4.1. No Difference in the Number of α-SMA$^+$ Cells in the Infarcted Hearts of Young vs. Old Mice

Cardiac fibroblasts transdifferentiate into myofibroblasts post-MI, leading to scar deposition and adverse remodeling (Bradshaw et al., 2010). Therefore, the number of myofibroblasts in myocardial tissue sections was compared between young and old mice at 14 days post-MI using α-SMA staining. Contrary to our expectations, there was no significant difference in the number of α-SMA$^+$ myofibroblasts between young and old mice in either the infarct or the border zone (Fig. 11).

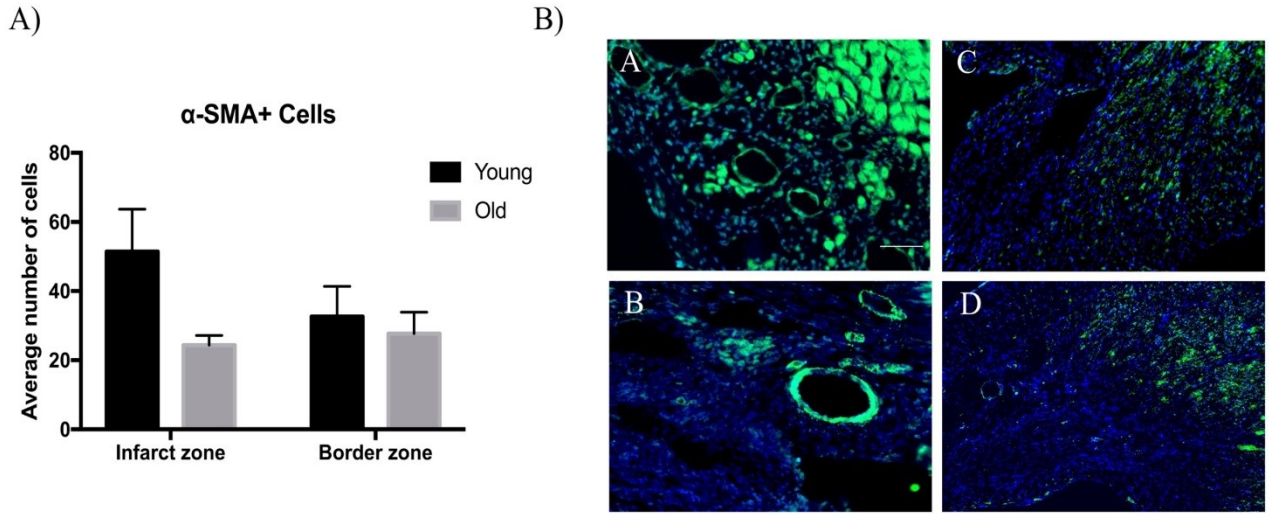

Figure 11. Immunostaining for α-SMA Positive Myofibroblasts at 14 Days Post-MI. A) Sections were stained to quantify the amount of α-SMA positive cells in the border and infarct region of the heart at 14 days post-MI (n=3). No statistical significance was observed. **B)** Immunostaining images α-SMA positive cells (green) and DAPI+ (blue) of the young infarct zone (A), old infarct zone (B), young border zone (C), and old border zone (D) (Scale bar = 100um).

3.5. There is no Change in Caspase-3-Mediated Apoptosis at 14-day Post-MI in Young and Old Myocardium

Cell apoptosis was identified in 14-day post-MI tissue sections using anti-caspase 3 antibody. Caspase 3 is a pro-apoptotic factor that has been found to be upregulated in cardiac hypertrophy, regulating fibroblast death in the myocardium (Fujiu & Nagai, 2014). Additionally, active-caspase 3 activity may have a tissue-specific effect that may be affected with age, predisposing the myocardium to further damage post-MI (Condorelli et al., 2001). At 14 days post-MI we did not see a difference between young and old mice in caspase-3-mediated apoptosis in the myocardium infarct and border zones (Fig. 12).

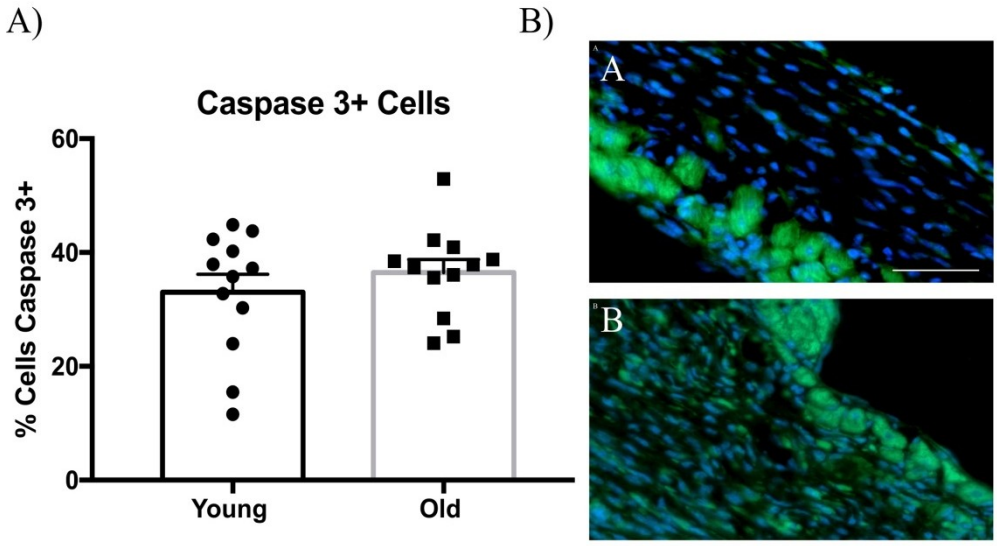

Figure 12. Active Caspase 3+ Cells in the Infarct and Border Zones in Young and Old Mice at 14 Days Post-MI. A) Total percentage active caspase 3+ cells in the infarct and border zones of 14-day post-MI tissue sections (n=4), determined by immunohistochemistry at 40× magnification. Data are represented as a mean SEM with no significance. **B)** Representative fluorescent images of active-caspase-3 (Green) and DAPI (blue) in a young mouse infarct zone (A) and old mouse infarct zone (B) at 14-days post-MI (Scale bar = 100um).

Discussion

Discussion

4. Post-MI Remodeling in the Aging Heart and the Role of Matricellular Proteins

Cardiovascular disease is one of the largest burdens on the aging population, with age being associated with the progressive deterioration in structure and function of the heart and vasculature. As such, aging is a risk factor for the development of CVD and related complications leading to MI. With the increase in life expectancy of the aging populations, it is of importance to understand the physiological changes that occur with age at a cellular and molecular level that can contribute to increased risk of CVD. Therefore, we examined the function of the CCN family of matricellular proteins in the cardiac ECM and their possible roles in regulating the repair and remodeling process post-MI in relation to old age. Notably, previous studies have revealed that the matricellular protein Nov has pro-angiogenic and anti-fibrotic functions in other inflammatory diseases (Marchal et al., 2015) and Wisp1 can increase vascular smooth muscle cells (VSMC) migration and cell survival in the vasculature and myocardium post-MI (Venkatachalam et al., 2009; Williams et al., 2016). However, the exact role in repair and remodeling post-MI remains to be fully elucidated. The aim of this project was to study the age-associated alterations of matricellular proteins Nov and Wisp1in the heart and to identify their potential role(s) in adverse remodeling and loss of function of the aging myocardium post-MI.

4.1. The Aged Mouse Myocardium Worsens Cardiac Function Post-MI

4.1.1. Cardiac Function is Reduced in Old Mice Compared to Young 2 Weeks Post-MI

Aging of the cardiovascular system is often associated with a decline in cardioprotective systems, structure, and function of the heart that can be observed at a cellular, extracellular and tissue level (Strait & Lakatta, 2012). We found that LVEF was reduced in aged female mice at 14 days post-MI compared to young female mice, suggesting that there may be a difference in post-MI repair/recovery with age. Following an ischemic event, the dynamic repair and remodeling process begins with the recruitment of inflammatory cells and progressive alterations to the extracellular environment. During the inflammatory phase, there can be a large amount of variability in the repair and remodeling process (Horn & Trafford, 2016; St. John Sutton & Sharpe, 2000). Specifically, the extent of the damage post-MI and the severity of the remodeling from LV dilation depend on the initial size of the infarct, as well as the characteristics of wound healing at a molecular level, including changes to the ECM. This can perhaps explain why a significant difference in LVEF between young and old mice was observed at 14 days and not at 2 and 7, days post-MI.

The reduced ability to recover post-MI in aging mice may be related to changes in the genome. Over a lifetime, genomic alterations can occur due to chemical damage, mutations and epigenetic alterations, especially with an accumulation of ROS in the myocardium. Recent evidence has shown that the accumulation of sporadic genomic mutations correlate to a higher likelihood to develop CVD, particularly with chromosomal damage, DNA deletions, single-nucleotide mutations and post-translational modifications (Cervelli, Borghini, Galli, & Andreassi, 2012). These alterations can affect the stability of the genome ultimately altering the

signaling pathways for tissue repair and remodeling, hence leading to a decrease in LVEF in old mice compared to young mice post-MI.

Despite a significant decrease in LVEF in old mice compared to young at 14 days post-MI, there was no significant difference in the size of the collagen-based scar. As explained above, an ischemic event can invoke a varying degree of repair responses, particularly in the early stages post-MI, based on the initial severity of the infarct and early cell responses (St. John Sutton & Sharpe, 2000; Talman & Ruskoaho, 2016). Functional and structural changes don't necessarily have to correlate and often times the injury and remodeling can affect the tissues differently, including ECM expansion and cell signaling within various areas of the heart. In addition to the infarct area, the border zone and remote myocardium can also be affected by MI and alter the heart function and physiological infarct healing (Chan et al., 2012; Randhawa, Bali, Virdi, & Jaggi, 2018; Richardson & Holmes, 2015). It is possible that older hearts have greater damage extending beyond the scar into these areas that contributed to the lower LVEF compared to the young mice. This would be an explanation for the lack of a difference in collagen content, yet the greater loss of LV function.

Given the importance of ECM remodeling in the post-MI repair process, we sought to identify differences in matricellular proteins between young and old mice. We observed a significant decrease in mRNA expression of many matricellular protein family members in healthy old mice hearts compared to healthy young mice hearts. This is what we had hypothesized since there are many known age-dependent alterations to the cardiac ECM (Bradshaw et al., 2010; De Castro Brás et al., 2014; Meschiari et al., 2017). Additionally, mRNA expression of the matricellular proteins Nov and Wisp1 was reduced in the infarct and border zones post-MI of old compared to young tissues. These results suggest that differences in the

content of matricellular proteins between young and old mice may play a role in the ability to recover after MI.

4.1.2. The Importance of CCN Proteins Post-MI

The roles that the CCN family of matricellular proteins play post-MI remains to be fully elucidated. Therefore, we examined the mRNA and protein expression of Nov/CCN3 and Wisp1/CCN4 in the young and old mouse heart post-MI. Overall, both the protein and mRNA expression of Nov and Wisp1 were decreased in the hearts of aged mice compared to young at 2, 7, and 14 days post-MI. However, the magnitude of the reduction in protein level did not always match the reduction in mRNA level. For example, we observed a ~4.5-fold reduction in Nov mRNA expression in the border zone of old hearts at 2 days post-MI compared to young; however, the corresponding protein levels were only decreased by about 2-fold. Due to many post-transcriptional and post-translational modifications, the mRNA and protein levels are not always in line with each other (Edvardsson, 2016; Tao et al., 2016). One reason for this is that microRNAs (miRNAs), which are short non-coding RNAs, are capable of regulating mRNA levels at the translation level (Cannell, Kong, & Bushell, 2008). This could be one explanation for why there are inconsistencies with the magnitude between RNA and protein levels. MiRNAs have the capability of activating gene expression or repressing gene expression, through direct and indirect mechanisms which are dependent on cell type and the cofactors within the environment. This results in a change of protein translation, through various post-translation modifications and binding to mRNA (Cannell et al., 2008; Orang, Safaralizadeh, & Kazemzadeh-Bavili, 2014). Given that miRNAs have also been shown to have altered expression in aged versus young mice (Kelm, Piell, Wang, & Cole, 2017), it is possible that a difference in

post-transcriptional or post-translational regulation is a factor contributing to the reduction in protein levels of Nov and Wisp1 post-MI in relation to mRNA levels.

With Nov, mRNA levels at 2, 7, and 14 days post-MI were significantly reduced in old mice compared to young, which was expected as the capacity of the ECM to maintain homeostasis following an injury is reduced in the aging myocardium (Meschiari et al., 2017). However, with protein expression, there was only a significant decrease in expression at 2 days post-MI in both infarct and border zone in old mice compared to young. Nov has been shown to regulate inflammation in chronic kidney disease (Marchal et al., 2015), suggesting a potential role in the regulation of post-MI inflammation, particularly at 2 days post-MI. Additionally, Nov may play a role in regulating cardiac fibroblasts and ECM production, since it has been shown to promote fibrosis in *in vitro* studies (Borkham-kamphorst et al., 2012; Ren et al., 2014).

For Wisp1, we observed a trend for increased mRNA expression at 2, 7, and 14 days post-MI in young mice compared to old. Transcription of Wisp1 is known to be regulated by histone deacetylases (HDACs) in the myocardium, which are elevated in CV related injuries (Wright, Herr, Brown, Kasiganesan, & Menick, 2018). This suggests there may be a greater increase in HDAC activity in young mice compared to old, possibly explaining the reduced Wisp1 transcription post-MI in the aged myocardium. There was also a significant reduction in Wisp1 protein expression in the old mouse border zone at 7 days post-MI and at 2 and, 14 days post-MI in the infarct area. Altogether, these results suggest that Nov and Wisp1 may play a role in inflammation and fibrosis post-MI, and that these functions are altered in old versus young mice leading to greater functional loss in the aged animals.

4.2. The Importance of Fibroblasts in the Myocardium Post-MI and Their Interactions with Nov and Wisp1

4.2.1 Activated Fibroblasts Show Increased Translation of Nov, While Stressed Fibroblasts Show an Increase in Wisp1 Transcription

Since it was observed that Nov and Wisp1 have altered expression post-MI *in vivo,* we decided to look at which cells may secrete these matricellular proteins *in vitro*, to provide us some potential insight into the source of their generation post-MI. Since Nov and Wisp1 have been linked to fibrosis (Königshoff et al., 2009; Marchal et al., 2015), we initially we looked into cardiac fibroblasts as a producer of these proteins. TGF-β is released in the myocardium as a stress response to ischemic injury leading to activation of cardiac fibroblasts and the release of various growth factors and cytokines to mediate the repair and remodeling process (Dobaczewski et al., 2011). When fibroblasts are activated to myofibroblasts with TGF-β stimulation, there is an upregulation of wound healing and cell-cell adhesion genes to promote repair (Tölle, Gaggioli, & Dengjel, 2018). In the present study, TGF-β treatment led to an increase in α-SMA expression at 48 hours, confirming the activation of cardiac fibroblasts to myofibroblasts *in vitro.* Notably, the increase in α-SMA expression coincided with a significant increase in Nov protein expression, with a similar trend observed for Wisp1. The increase of Nov observed in activated cardiac fibroblasts matches the result of another study where human palatal fibroblasts were shown to produce Nov upon activation *in vitro* (Ren et al., 2014). When cardiac fibroblasts were cultured under stress conditions of serum starvation and hypoxia (1% O_2), there was a significant increase in Wisp1 production. Wisp1 expression is controlled by the Wnt signaling pathway, which is known to be upregulated in many fibrotic diseases, mediating the function of various phenotypes of fibroblasts and other cell types in the myocardium (Königshoff et al., 2009). Given that Wnt signaling also controls cardiac fibroblast function post-MI, mediating

differentiation, adhesion and proliferation (Daskalopoulos, Janssen, & Blankesteijn, 2013), it is not surprising that we observed increased Wisp1 levels in this study.

As Nov and Wisp1 have been linked with regulating inflammation, we also investigated their production in macrophages. Macrophages are not only the key players in the inflammatory phase post-MI, but they also mediate tissue remodeling and regeneration. With the significant difference observed in Nov and Wisp1 protein expression at 2 days post-MI *in vivo*, representing a time point near the transition from inflammatory to proliferative phases, we expected to see an altered expression of Nov and Wisp1 upon polarization of M0 macrophages to the M1 or M2 phenotype. However, looking at isolated macrophages *in vitro* we found no significant change upon M1 or M2 stimulation. There was a trend for reduced Nov and Wisp1 levels in the pro-inflammatory M1 phenotype compared to the anti-inflammatory M2 phenotype, but it did not reach statistical significance. As mentioned earlier, Wisp1 is involved in the Wnt signaling pathways. Since Wnt signaling is active during inflammation through interaction between cardiomyocytes and macrophages (Meyer et al., 2017), we predicted that Wisp1 might be upregulated in macrophages, but this was not what we observed. There may be conditions *in vivo* that were not present in our *in vitro* culture conditions that may account for the lack of change in expression. Altogether, our results are not conclusive in determining if macrophages are a potential source of Nov and Wisp1 in the infarcted myocardium.

4.2.2 Exogenous Nov and Wisp1 Affect the Functions of Cardiac Fibroblasts *in Vitro*

With the knowledge that fibroblasts play a key role in the repair and remodeling process post-MI, we looked at the exogenous effects of Nov and Wisp1. We found that fibroblasts treated with either Nov or Wisp1 for 48 hours, in the presence and absence of TGF-β, exhibited

increased proliferation. These data suggest that Nov and Wisp1 may be involved in stimulating cardiac fibroblast proliferation post-MI. TGF-β also stimulates the transdifferentiation of fibroblasts to myofibroblasts, which are highly proliferative post-MI (X. Fu et al., 2018). Proliferation of fibroblasts in the myocardium post-MI involves many exogenous inducers and signaling networks (Chistiakov et al., 2016), and these two matricellular proteins may also be involved through ECM communication. Additionally, previous work has demonstrated that the presence of Nov correlates to an increase in human palatal fibroblast numbers, mediating fibrosis (Ren et al., 2014) and Wisp1 has previously been shown to increase fibroblast proliferation in cardiac fibroblasts *in vitro* (Venkatachalam et al., 2009). These findings validate our results of increasing cardiac fibroblast proliferation.

Since exogenous Nov and Wisp1 were found to increase cardiac fibroblast proliferation in regular growth conditions, we decided to look at how it affects cell death of cardiac fibroblasts under stressed conditions, consisting of hypoxia and serum deprivation. The data showed that both Nov and Wisp1 treated fibroblasts had increased viability, suggesting a potential pro-survival role on cardiac fibroblasts. Although using a different cardiac cell type, Wisp1 has been shown to mediate cardiomyocyte death *in vitro* through a TNF-α signaling pathway that is integrin mediated (Venkatachalam et al., 2009). Similarly, a survival role for Nov on fibroblasts has not yet been reported, however other members of the CCN family of matricellular proteins have been shown to regulate cell survival in the myocardium of embryos (Krupska, Bruford, & Chaqour, 2015; Lau, 2016; Mo & Lau, 2006). Together, these *in vitro* observations for Nov and Wisp1 on activated cardiac fibroblasts demonstrate a potential role for their function in regulating post-MI remodeling. Their functions *in vivo* should be determined to identify how they mediate fibroblasts in repair and remodeling post-MI.

4.3. Presence of Myofibroblasts Post-MI and Apoptosis

Myofibroblasts in the myocardium play an important role with ECM deposition and maintaining structural integrity of the heart following MI. They express the contractile protein α-SMA, allowing the cells to assist in stabilizing the ventricle post-MI during the proliferative phase (Weber et al., 2013). To determine if there is an age associated difference in myofibroblast number, we looked at 14 days post-MI but did not see a significant difference. However, there was a trend observed for increased numbers of α-SMA positive myofibroblasts in the young infarct and border zones post-MI compared to old. It has been reported that the matrifibrocyte form of fibroblast is pre-dominant in the myocardium after 10 days post-MI, and this phenotype lacks the presence of contractile proteins (X. Fu et al., 2018). Thus, perhaps the 14-day time-point was too late to observe differences in the number of α-SMA positive myofibroblasts between aged and young mice post-MI.

In order to identify the amount of cell death occurring post-MI in the myocardium, we looked at the presence of active caspase 3, a marker of apoptosis, at 14 days post-MI. Reparative fibrosis occurs in the myocardium in locations where myocytes undergo apoptosis and necrotic death (Barbara, 2016), and active caspase 3 expression has been correlated with the extent of infarct expansion and loss of function (Condorelli et al., 2001). There was no observed difference in the number of caspase 3 positive cells in the infarct or border zone of young mice compared to old. Since the peak in caspase 3 mediated apoptosis occurs during the initial hours to days post-MI, it may be of use to look at the earlier time-points post-MI or other forms of cell death pathways at 14 days post-MI.

4.4. Future Directions

While this study examined the age-associated effects of cardiac function, there are a still a few obstacles within age-related studies to be addressed in the future. For example, age-associated effects accumulate over time, and female hormones may affect cellular mechanisms involved in repair and remodeling. This could make it more critical to identify the best suitable age to select when engaging in age-related research. For example, D. Belsky et al., previously determined a method to quantify the pace of aging in young humans based on their variable biological aging and physiological deterioration (Belsky et al., 2015). By studying the progressive deterioration through the aging mouse at a molecular level, more evidence may be found indicating why there is a reduction in LVEF in old mice, compared to young post-MI. Additionally, many circulating hormones are capable of traveling through the extracellular space, and interacting with the molecules and ECM components in the myocardium (Valiente-Alandi, Schafer, & Blaxall, 2016). Our study used female mice, which are producing estrogen and progesterone at various levels depending on their age and reproductive and cycle status. There is much research indicating sex differences and hormone levels may affect the manifestation of CVD, including potential cardioprotective effects on the heart, yet the exact mechanism remains unknown (Luo & Kyung Kim, 2016). For example, the loss of estrogen following menopause has been linked to the late onset of CVD in women compared to men (Bhupathy, Haines, & Leinwand, 2010). With this in mind, it would have been beneficial to determine the levels of estrogen in the mice used in this study, to see if this had any correlation to the heart's ability to recover post-MI.

The next step in this project would be to determine the *in vivo* localization of Nov and Wisp1 using *in situ* hybridization and immunohistochemistry. This would be helpful to identify

what are the primary cell types producing these matricellular proteins *in vivo*, which could then be targeted to help improve the post-MI environment and increase repair and regeneration.

Another limitation of the present study is that we did not study cardiomyocytes, which are another main cell type present in the myocardium. This is due to the fact that cardiomyocytes are hard to culture unless they are in their neonatal state, along with the knowledge that matricellular proteins are more highly expressed in the embryotic stages. Therefore, in the future we would like to look at their expression profiles in that cell type if a cell separation technique were to be developed that allowed for the isolation of cardiomyocytes from the heart without the need for culture steps. Additionally, it would be of use to determine the *in vitro* effects of Nov and Wisp1 on cells cultured from aged animals to see if age affects some of their specific roles and functions.

Once the exact roles of Nov and Wisp1 are determined *in vivo* and we know more about how they mediate the repair and remodeling process, we may be able to exploit their specific functions to ameliorate healing post-MI, thereby attenuating adverse tissue remodeling and preserving cardiac function in the aging population. For example, knowledge about matricellular proteins, such as Nov and Wisp1, may be applied to improve biomaterial therapies that are being developed to treat MI. Biomaterial therapies have been shown to improve the post-MI ECM environment leading to superior repair and cardiac function. By integrating Nov and Wisp1 into such material therapies, we may be able to exploit their pro-angiogenic and anti-fibrotic properties to better preserve myocardial tissue post-MI, which could lead to future clinical use in treating MI in the aged population.

Conclusion

Conclusion

5. There is an Age-Associated Difference in the Expression of Nov and Wisp1 Post-MI

We showed that there is an age-associated difference in the expression of matricellular proteins Nov and Wisp1 in healthy and MI mice. This may be associated with the decreased cardiac function of old mice compared to young mice post-MI, which suggests a potential role of Nov and Wisp1 in the repair and remodeling process. A better understanding of Nov and Wisp1 function in aging and post-MI repair may help identify novel therapeutic targets for limiting damage post-MI and improving myocardial repair and heart function.

References

References

6. References

Asif, M., Egan, J., Vasan, S., Jyothirmayi, G., Masurekar, M., Lopez, S., … Regan, T. (2000). An advanced glycation endproduct cross-link breaker can reverse age-related increases in mycardial stiffness. *PNAS*, *97*(4), 2809–2013.

Aurora, A. B., Porrello, E. R., Tan, W., Mahmoud, A. I., Hill, J. A., Bassel-Duby, R., … Olson, E. N. (2014). Macrophages are required for neonatal heart regeneration. *Journal of Clinical Investigation*, *124*(3), 1382–1392. https://doi.org/10.1172/JCI72181

Bai, T., Chen, C.-C., & Lau, L. F. (2010). Matricellular protein CCN1 activates a proinflammatory genetic program in murine macrophages. *Journal of Immunology (Baltimore, Md. : 1950)*, *184*, 3223–3232. https://doi.org/10.4049/jimmunol.0902792

Barbara, W. (2016). Fibrosis of extracellular matrix is related to the duration of the disease but is unrelated to the dynamics of collagen metabolism in dilated cardiomyopathy, 941–949. https://doi.org/10.1007/s00011-016-0977-3

Belsky, D. W., Caspi, A., Houts, R., Cohen, H. J., Corcoran, D. L., Danese, A., … Moffitt, T. E. (2015). Quantification of biological aging in young adults. *Proceedings of the National Academy of Sciences*, *112*(30), E4104–E4110. https://doi.org/10.1073/pnas.1506264112

Benjamin, E. J., Blaha, M. J., Chiuve, S. E., Cushman, M., Das, S. R., Deo, R., … Muntner, P. (2017). *Heart Disease and Stroke Statistics—2017 Update: A Report From the American Heart Association*. *Circulation* (Vol. 135). https://doi.org/10.1161/CIR.0000000000000485

Bergmann, M. W. (2010). WNT signaling in adult cardiac hypertrophy and remodeling: Lessons learned from cardiac development. *Circulation Research*, *107*(10), 1198–1208. https://doi.org/10.1161/CIRCRESAHA.110.223768

Bhupathy, P., Haines, C. D., & Leinwand, L. A. (2010). Influences of sex hormones and phytoestrogens on heart disease in men and women. *Womens Health*, *6*(1), 77–95. https://doi.org/10.2217/whe.09.80.Influence

Blackburn, N. J. R., Sofrenovic, T., Kuraitis, D., Ahmadi, A., McNeill, B., Deng, C., … Suuronen, E. J. (2015). Timing underpins the benefits associated with injectable collagen biomaterial therapy for the treatment of myocardial infarction. *Biomaterials*, *39*, 182–192. https://doi.org/10.1016/j.biomaterials.2014.11.004

Bonaventura, A., Montecucco, F., & Dallegri, F. (2016). Cellular recruitment in myocardial ischaemia/reperfusion injury. *European Journal of Clinical Investigation*, *46*(6), 590–601. https://doi.org/10.1111/eci.12633

Borkham-kamphorst, E., Roeyen, C. R. Van, & Leur, E. Van De. (2012). CCN3 / NOV small interfering RNA enhances fibrogenic gene expression in primary hepatic stellate cells and cirrhotic fat storing cell line CFSC, 11–25. https://doi.org/10.1007/s12079-011-0141-3

Bornstein, P. (2009). Matricellular proteins: An overview. *Journal of Cell Communication and Signaling*, *3*(3–4), 163–165. https://doi.org/10.1007/s12079-009-0069-z

Bradshaw, A. D., Baicu, C. F., Rentz, T. J., Van Laer, A. O., Bonnema, D. D., & Zile, M. R. (2010). Age-dependent alterations in fibrillar collagen content and myocardial diastolic function: role of SPARC in post-synthetic procollagen processing. *American Journal of*

Physiology. Heart and Circulatory Physiology, *298*(2), H614–H622. https://doi.org/10.1152/ajpheart.00474.2009

Cannell, I. G., Kong, Y. W., & Bushell, M. (2008). How do microRNAs regulate gene expression? *Biochemical Society Transactions*, *36*(6), 1224–1231. https://doi.org/10.1042/BST0361224

Cervelli, T., Borghini, A., Galli, A., & Andreassi, M. G. (2012). DNA damage and repair in atherosclerosis: Current insights and future perspectives. *International Journal of Molecular Sciences*, *13*(12), 16929–16944. https://doi.org/10.3390/ijms131216929

Chan, W., Duffy, S. J., White, D. A., Gao, X. M., Du, X. J., Ellims, A. H., … Taylor, A. J. (2012). Acute left ventricular remodeling following myocardial infarction: Coupling of regional healing with remote extracellular matrix expansion. *JACC: Cardiovascular Imaging*, *5*(9), 884–893. https://doi.org/10.1016/j.jcmg.2012.03.015

Chen, C. C., & Lau, L. F. (2009). Functions and mechanisms of action of CCN matricellular proteins. *International Journal of Biochemistry and Cell Biology*, *41*(4), 771–783. https://doi.org/10.1016/j.biocel.2008.07.025

Chen, W., & Frangogiannis, N. G. (2013). Fibroblasts in post-infarction inflammation and cardiac repair. *Biochim Biophys Acta.*, *1833*(4), 945–953. https://doi.org/10.1016/j.bbamcr.2012.08.023.Fibroblasts

Chistiakov, D. A., Orekhov, A. N., & Bobryshev, Y. V. (2016). The role of cardiac fibroblasts in post-myocardial heart tissue repair. *Experimental and Molecular Pathology*, *101*(2), 231–240. https://doi.org/10.1016/j.yexmp.2016.09.002

Colston, J. T., de la Rosa, S. D., Koehler, M., Gonzales, K., Mestril, R., Freeman, G. L., … Chandrasekar, B. (2007). Wnt-induced secreted protein-1 is a prohypertrophic and profibrotic growth factor. *American Journal of Physiology-Heart and Circulatory Physiology*, *293*(3), H1839–H1846. https://doi.org/10.1152/ajpheart.00428.2007

Condorelli, G., Roncarati, R., Ross, J., Pisani, A., Stassi, G., Todaro, M., … Croce, C. M. (2001). Heart-targeted overexpression of caspase3 in mice increases infarct size and depresses cardiac function. *Proceedings of the National Academy of Sciences*, *98*(17), 9977–9982. https://doi.org/10.1073/pnas.161120198

Daskalopoulos, E. P., Janssen, B. J. A., & Blankesteijn, W. M. (2013). Targeting wnt signaling to improve wound healing after myocardial infarction. In *Methods in Molecular Biology* (Vol. 1037, pp. 355–380). https://doi.org/10.1007/978-1-62703-505-7_21

De Castro Brás, L. E., Toba, H., Baicu, C. F., Zile, M. R., Weintraub, S. T., Lindsey, M. L., & Bradshaw, A. D. (2014). Age and SPARC change the extracellular matrix composition of the left ventricle. *BioMed Research International*, *2014*. https://doi.org/10.1155/2014/810562

De Haan, J. J., Smeets, M. B., Pasterkamp, G., & Arslan, F. (2013). Danger signals in the initiation of the inflammatory response after myocardial infarction. *Mediators of Inflammation*, *2013*. https://doi.org/10.1155/2013/206039

Dobaczewski, M., Chen, W., & Frangogiannis, N. G. (2011). Transforming Growth Factor (TGF)-B signaling in cardiac remodeling. *J Mol Cell Cardiol*, *51*(4), 600–606. https://doi.org/10.1016/j.yjmcc.2010.10.033.Transforming

Dobaczewski, M., Gonzalez-Quesada, C., & Frangogiannis, N. G. (2010). The extracellular matrix as a modulator of the inflammatory and reparative response following myocardial infarction. *Journal of Molecular and Cellular Cardiology*, *48*(3), 504–511. https://doi.org/10.1016/j.yjmcc.2009.07.015

Edvardsson, M. (2016). *A Comparative Study of qPCR , Western Blot and Mass Spectrometry for the Estimation of Protein Concentrations*. *KTH Royal Institute of Technology*.

Elias, M. F., Elias, P. K., Sullivan, L. M., Wolf, P. A., & D'Agostino, R. B. (2005). Obesity, diabetes and cognitive deficit: The Framingham Heart Study. *Neurobiology of Aging*, *26*(SUPPL.). https://doi.org/10.1016/j.neurobiolaging.2005.08.019

Fan, D., Takawale, A., Lee, J., & Kassiri, Z. (2012). Cardiac fibroblasts , fibrosis and extracellular matrix remodeling in heart disease, 1–13.

Fang, L., Murphy, A. J., & Dart, A. M. (2017). A clinical perspective of anti-fibrotic therapies for cardiovascular disease. *Frontiers in Pharmacology*, *8*(APR), 1–8. https://doi.org/10.3389/fphar.2017.00186

Frangogiannis, N. G. (2014). The inflammatory response in myocardial injury, repair, and remodelling. *Nature Reviews Cardiology*, *11*(5), 255–265. https://doi.org/10.1038/nrcardio.2014.28

Franogogiannis, N. G. (2011). Matricellular proteins in cardiac inflammation and fibrosis. *Respiration and Circulation*, *59*(11), 1077–1082. https://doi.org/10.1152/physrev.00008.2011

Fu, W., Wang, W. E., & Zeng, C. (2018). Wnt signaling pathways in myocardial infarction and the therapeutic effects of Wnt pathway inhibitors. *Acta Pharmacologica Sinica*, (January), 1–4. https://doi.org/10.1038/s41401-018-0060-4

Fu, X., Khalil, H., Kanisicak, O., Boyer, J. G., Vagnozzi, R. J., Maliken, B. D., … Molkentin, J. D. (2018). Specialized fibroblast differentiated states underlie scar formation in the infarcted mouse heart Graphical abstract Find the latest version : Specialized fibroblast differentiated states underlie scar formation in the infarcted mouse heart, *128*(5), 2127–2143. https://doi.org/10.1172/JCI98215

Fujiu, K., & Nagai, R. (2014). Fibroblast-mediated pathways in cardiac hypertrophy. *Journal of Molecular and Cellular Cardiology*, *70*, 64–73. https://doi.org/10.1016/j.yjmcc.2014.01.013

Furtado, M. B., Nim, H. T., Boyd, S. E., & Rosenthal, N. A. (2016). View from the heart: cardiac fibroblasts in development, scarring and regeneration. *Development*, *143*(3), 387–397. https://doi.org/10.1242/dev.120576

Gazoti Debessa, C. R., Mesiano Maifrino, L. B., & Rodrigues de Souza, R. (2001). Age related changes of the collagen network of the human heart. *Mechanisms of Ageing and Development*, *122*(10), 1049–1058. https://doi.org/10.1016/S0047-6374(01)00238-X

Horn, M. A., & Trafford, A. W. (2016). Aging and the cardiac collagen matrix: Novel mediators of fibrotic remodelling. *Journal of Molecular and Cellular Cardiology*, *93*, 175–185. https://doi.org/10.1016/j.yjmcc.2015.11.005

Hulsmans, M., Sam, F., & Nahrendorf, M. (2016). Monocyte and Macrophage Contributions to Cardiac Remodeling. *J Mol Cell Cardiol.*, (93), 149–155. https://doi.org/10.1021/acschemneuro.5b00094.Serotonin

Kelm, N. Q., Piell, K. M., Wang, E., & Cole, M. P. (2017). MicroRNAs as Predictive Biomarkers for Myocardial Injury in Aged Mice Following Myocardial Infarction. *Journal of Cellular Physiology*, (November), 1–8. https://doi.org/10.1002/jcp.26283

Königshoff, M., Kramer, M., Balsara, N., Wilhelm, J., Amarie, O. V., Jahn, A., … Eickelberg, O. (2009). WNT1-inducible signaling protein – 1 mediates pulmonary fibrosis in mice and is upregulated in humans with idiopathic pulmonary fibrosis, *119*(4). https://doi.org/10.1172/JCI33950DS1

Krijnen, P. A. J., Nijmeijer, R., Meijer, C. J. L. M., Visser, C. A., Hack, C. E., & Niessen, H. W.

M. (2002). Apoptosis in myocardial ischaemia and infarction. *Journal of Clinical Pathology*, *55*(11), 801–811. https://doi.org/10.1136/jcp.55.11.801

Krupska, I., Bruford, E. A., & Chaqour, B. (2015). Eyeing the Cyr61/CTGF/NOV (CCN) group of genes in development and diseases: highlights of their structural likenesses and functional dissimilarities. *Human Genomics*, *9*(1), 1–13. https://doi.org/10.1186/s40246-015-0046-y

Lajiness, J. D., & Conway, S. J. (2014). Origin, development, and differentiation of cardiac fibroblasts. *Journal of Molecular and Cellular Cardiology*, *70*(317), 2–8. https://doi.org/10.1016/j.yjmcc.2013.11.003

Lau, L. F. (2012). CCN1 and CCN2: Blood brothers in angiogenic action. *Journal of Cell Communication and Signaling*, *6*(3), 121–123. https://doi.org/10.1007/s12079-012-0169-z

Lau, L. F. (2016). Cell surface receptors for CCN proteins. *Journal of Cell Communication and Signaling*, *10*(2), 121–127. https://doi.org/10.1007/s12079-016-0324-z

Leask, A., & Abraham, D. J. (2006). All in the CCN family: essential matricellular signaling modulators emerge from the bunker. *Journal of Cell Science*, *119*(23), 4803–4810. https://doi.org/10.1242/jcs.03270

Leor, J., Palevski, D., Amit, U., & Konfino, T. (2016). Macrophages and regeneration: Lessons from the heart. *Seminars in Cell and Developmental Biology*, *58*, 26–33. https://doi.org/10.1016/j.semcdb.2016.04.012

Lin, C. G., Chen, C. C., Leu, S. J., Grzeszkiewicz, T. M., & Lau, L. F. (2005). Integrin-dependent functions of the angiogenic inducer NOV (CCN3): Implication in wound healing. *Journal of Biological Chemistry*, *280*(9), 8229–8237. https://doi.org/10.1074/jbc.M404903200

Lin, C., Leu, S., Chen, N., Tebeau, C. M., Lin, S., Yeung, C., & Lau, L. F. (2003). CCN3 (NOV) Is a Novel Angiogenic Regulator of the CCN Protein Family, *3*(312).

Lindsey, M. L., Saucerman, J. J., & DeLeon-Pennell, K. Y. (2016). Knowledge gaps to understanding cardiac macrophage polarization following myocardial infarction. *Biochimica et Biophysica Acta - Molecular Basis of Disease*, *1862*(12), 2288–2292. https://doi.org/10.1016/j.bbadis.2016.05.013

Liu, H., Liu, H., Lv, L., Ma, K., Wen, Y., Chen, L., & Liu, B. (2017). CCN3 suppresses TGF-β1-induced extracellular matrix accumulation in human mesangial cells in vitro. *Acta Pharmacologica Sinica*, 1–8. https://doi.org/10.1038/aps.2017.87

Luo, T., & Kyung Kim, J. (2016). The Role of Estrogen and Estrogen Receptors on Cardiomyocytes: An Overview. *Canadian Journal of Cardiology*, *32*(8), 923–930. https://doi.org/10.1016/j.clinbiochem.2015.06.023.Gut-Liver

Ma, Y., De Castro Bras, L. E., Toba, H., Iyer, R. P., Hall, M. E., Winniford, M. D., … Lindsey, M. L. (2014). Myofibroblasts and the extracellular matrix network in post-myocardial infarction cardiac remodeling. *Pflugers Archiv European Journal of Physiology*, *466*(6), 1113–1127. https://doi.org/10.1007/s00424-014-1463-9

Marchal, P. O., Kavvadas, P., Abed, A., Kazazian, C., Authier, F., Koseki, H., … Chadjichristos, C. E. (2015). Reduced NOV/CCN3 expression limits inflammation and interstitial renal fibrosis after obstructive nephropathy in mice. *PLoS ONE*, *10*(9), 1–12. https://doi.org/10.1371/journal.pone.0137876

McNeill, B., Vulesevic, B., Ostojic, A., Ruel, M., & Suuronen, E. J. (2015). Collagen matrix-induced expression of integrin αVβ3 in circulating angiogenic cells can be targeted by matricellular protein CCN1 to enhance their function. *FASEB Journal*, *29*(4), 1198–1207.

https://doi.org/10.1096/fj.14-261586
Meschiari, C. A., Ero, O. K., Pan, H., Finkel, T., & Lindsey, M. L. (2017). The impact of aging on cardiac extracellular matrix. *GeroScience*, *39*(1), 7–18. https://doi.org/10.1007/s11357-017-9959-9
Mewton, N., Liu, C. Y., Croisille, P., Bluemke, D., & Lima, J. A. C. (2011). Assessment of myocardial fibrosis with cardiovascular magnetic resonance. *Journal of the American College of Cardiology*, *57*(8), 891–903. https://doi.org/10.1016/j.jacc.2010.11.013
Meyer, I. S., Jungmann, A., Dieterich, C., Zhang, M., Lasitschka, F., Werkmeister, S., … Leuschner, F. (2017). The cardiac microenvironment uses non- canonical WNT signaling to activate monocytes after myocardial infarction. *EMBO Molecular Medicine*, *9*(9), 1279–1293. https://doi.org/10.15252/emmm.201707565
Mo, F. E., & Lau, L. F. (2006). The matricellular protein CCN1 is essential for cardiac development. *Circulation Research*, *99*(9), 961–969. https://doi.org/10.1161/01.RES.0000248426.35019.89
Nah, D.-Y., & Rhee, M.-Y. (2009). The Inflammatory Response and Cardiac Repair After Myocardial Infarction. *Korean Circulation Journal*, *39*(10), 393. https://doi.org/10.4070/kcj.2009.39.10.393
Orang, A. V., Safaralizadeh, R., & Kazemzadeh-Bavili, M. (2014). Mechanisms of miRNA-mediated gene regulation from common downregulation to mRNA-specific upregulation. *International Journal of Genomics*, *2014*(June 2013). https://doi.org/10.1155/2014/970607
Paneni, F., Canestro, C. D., Libby, P., Luscher, T. F., & Camici, G. G. (2017). The Aging Cardiovascular System: Understanding it at the Cellular and Clinical Levels. *Journal of the American College of Cardiology*, *69*(15). https://doi.org/10.1016/j.jacc.2017.01.064
Perbal, A., & Perbal, B. (2016). The CCN family of proteins: a 25th anniversary picture. *Journal of Cell Communication and Signaling*, *10*(3), 177–190. https://doi.org/10.1007/s12079-016-0340-z
Perbal, B. (2018). The concept of the CCN protein family revisited : a centralized coordination network, *5*, 3–12. https://doi.org/10.1007/s12079-018-0455-5
Prabhu, S. D., & Frangogiannis, N. G. (2016). The biological basis for cardiac repair after myocardial infarction. *Circulation Research*, *119*(1), 91–112. https://doi.org/10.1161/CIRCRESAHA.116.303577
Randhawa, P. K., Bali, A., Virdi, J. K., & Jaggi, A. S. (2018). Conditioning-induced cardioprotection: Aging as a confounding factor. *The Korean Journal of Physiology & Pharmacology*, *22*(5), 467. https://doi.org/10.4196/kjpp.2018.22.5.467
Ren, Z., Hou, Y., Ma, S., Tao, Y., Li, J., Cao, H., & Ji, L. (2014). Effects of CCN3 on fibroblast proliferation, apoptosis and extracellular matrix production. *Int J Mol Med*, *33*(6), 1607–1612. https://doi.org/10.3892/ijmm.2014.1735
Richardson, W. J., & Holmes, J. W. (2015). Why Is Infarct Expansion Such an Elusive Therapeutic Target? *Journal of Cardiovascular Translational Research*, *8*(7), 421–430. https://doi.org/10.1007/s12265-015-9652-2
Schellings, M. W. M., Pinto, Y. M., & Heymans, S. (2004). Matricellular proteins in the heart: Possible role during stress and remodeling. *Cardiovascular Research*, *64*(1), 24–31. https://doi.org/10.1016/j.cardiores.2004.06.006
Shinde, A. V., & Franogogiannis, N. G. (2014). Fibroblasts in myocardial infarction: a role in inflammation and repair. *J Mol Cell Cardiol.*, (0), 74–82. https://doi.org/10.1016/j.yjmcc.2013.11.015.Fibroblasts

Souders, C. A., Bowers, S. L. K., & Baudino, T. A. (2009). Cardiac fibroblast: The renaissance cell. *Circulation Research*, *105*(12), 1164–1176. https://doi.org/10.1161/CIRCRESAHA.109.209809

St. John Sutton, M. G., & Sharpe, N. (2000). Left Ventricular Remodeling After Myocardial Infarction Pathophysiology and Therapy. *Circulation*, *101*, 2981–2988. https://doi.org/10.1161/01.CIR.101.25.2981

Stephens, S., Palmer, J., Konstantinova, I., Pearce, A., Jarai, G., & Day, E. (2015). A functional analysis of Wnt inducible signalling pathway protein −1 (WISP-1/CCN4). *Journal of Cell Communication and Signaling*, *9*(1), 63–72. https://doi.org/10.1007/s12079-015-0267-9

Stewart, S. (2003). Heart failure and the aging population: an increasing burden in the 21st century? *Heart*, *89*(1), 49–53. https://doi.org/10.1136/heart.89.1.49

Strait, J., & Lakatta, E. (2012). Aging-associated cardiovascular changes and their relationship to heart failure. *Heart Failure Clinics*, *8*(1), 143–164. https://doi.org/10.1016/j.hfc.2011.08.011.Aging-associated

Sun, Y. A. O., Zhang, J. Q., Zhang, J., & Lamparter, S. (2000). Cardiac remodeling by fibrous tissue after infarction in rats, (Mi). https://doi.org/10.1067/mlc.2000.105971

Takagawa, J., Zhang, Y., Wong, M. L., Sievers, R. E., Kapasi, N. K., Wang, Y., … Matthew, L. (2009). Myocardial Infarct Size Measurment in the Mouse Chronic Infarction Model: Comparison of Area- and Length-Based Approaches. *Journal of Applied Physiology*, *102*(6), 2104–2111. https://doi.org/10.1152/japplphysiol.00033.2007.Myocardial

Talman, V., & Ruskoaho, H. (2016). Cardiac fibrosis in myocardial infarction — from repair and remodeling to regeneration. *Cell and Tissue Research*, 563–581. https://doi.org/10.1007/s00441-016-2431-9

Tao, J., Wang, Y., Abudoukelimu, M., Yang, Y., Li, X., Xie, X., … Ma, Y. (2016). Association of genetic variations in the Wnt signaling pathway genes with myocardial infarction susceptibility in Chinese Han population. *Oncotarget*, *7*(33), 52740–52750. https://doi.org/10.18632/oncotarget.10401

Thygesen, K., Alpert, J. S., & White, H. D. (2007). Universal definition of myocardial infarction. *European Heart Journal*, *28*(20), 2525–2538. https://doi.org/10.1093/eurheartj/ehm355

Tölle, R. C., Gaggioli, C., & Dengjel, J. (2018). Three-dimensional cell culture conditions affect the proteome of cancer-associated fibroblasts. *Journal of Proteome Research*, acs.jproteome.8b00237. https://doi.org/10.1021/acs.jproteome.8b00237

Twigg, S. M. (2018). Regulation and bioactivity of the CCN family of genes and proteins in obesity and diabetes. *Journal of Cell Communication and Signaling*, *12*(1), 359–368. https://doi.org/10.1007/s12079-018-0458-2

Valiente-Alandi, I., Schafer, A. E., & Blaxall, B. C. (2016). Extracellular matrix-mediated cellular communication in the heart. *J Mol Cell Cardiol.*, *91*(1), 228–237. https://doi.org/10.5993/AJHB.40.1.1.The

Van Linthout, S., Miteva, K., & Tschöpe, C. (2014). Crosstalk between fibroblasts and inflammatory cells. *Cardiovascular Research*, *102*(2), 258–269. https://doi.org/10.1093/cvr/cvu062

Venkatachalam, K., Venkatesan, B., Valente, A. J., Melby, P. C., Nandish, S., Reusch, J. E. B., … Chandrasekar, B. (2009). WISP1, a pro-mitogenic, pro-survival factor, mediates tumor necrosis factor-a (TNF-a)-stimulated cardiac fibroblast proliferation but inhibits TNF-a-induced cardiomyocyte death. *Journal of Biological Chemistry*, *284*(21), 14414–14427. https://doi.org/10.1074/jbc.M809757200

Weber, K. T., Sun, Y., Bhattacharya, S. K., Ahokas, R. a, & Gerling, I. C. (2013). Myofibroblast-mediated mechanisms of pathological remodelling of the heart. *Nature Reviews. Cardiology*. https://doi.org/10.1038/nrcardio.2012.158

Williams, H., Mill, C. A. E., Monk, B. A., Hulin-Curtis, S., Johnson, J. L., & George, S. J. (2016). Wnt2 and WISP-1/CCN4 Induce Intimal Thickening via Promotion of Smooth Muscle Cell Migration. *Arteriosclerosis, Thrombosis, and Vascular Biology*, *36*(7), 1417–1424. https://doi.org/10.1161/ATVBAHA.116.307626

Wolf, N., Yang, W., Dunk, C. E., Gashaw, I., Lye, S. J., Ring, T., … Gellhaus, A. (2010). Regulation of the matricellular proteins CYR61 (CCN1) and NOV (CCN3) by hypoxia-inducible factor-1?? and transforming-growth factor-??3 in the human trophoblast. *Endocrinology*, *151*(6), 2835–2845. https://doi.org/10.1210/en.2009-1195

Wright, L. H., Herr, D. J., Brown, S. S., Kasiganesan, H., & Menick, D. R. (2018). Angiokine Wisp-1 is increased in myocardial infarction and regulates cardiac endothelial signaling, *3*(4), 1–22.

Yeger, H., & Perbal, B. (2016). CCN family of proteins: critical modulators of the tumor cell microenvironment. *Journal of Cell Communication and Signaling*, 1–12. https://doi.org/10.1007/s12079-016-0346-6

Appendices

Appendices

7. Appendix A – Supplemental Data

7.1. Preparing Recombinant Nov and Wisp1 used for in vitro experiments

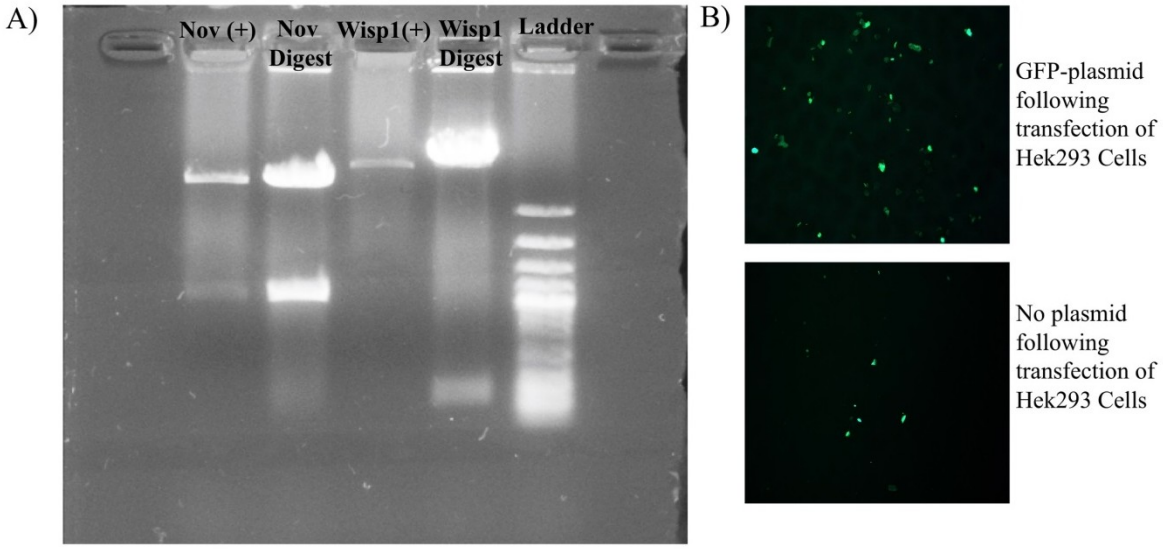

Figure 13. DH5α Bacterial Transformation and Hek293 Cell Transfection of Nov and Wisp1. Plasmid DNA of Nov and Wisp1 were used to transform bacterial cells using the heat shock method. **A)** A DNA digest was performed on DNA isolated from DH5a cell culture following a Maxi-Prep using BamHI and NotI (Digested for 60 minutes at 37 degrees). 15 uL of digested sample was run using gel electrophoresis. The Nov and Wisp1 digested DNA was used for Hek293 cell transfection. **B)** Transfection was performed using Lipofectamine 2000 and a GFP-control plasmid was used to ensure the transfection was successful. The large number of GFP-positive cells visualized using fluorescent microscopy compared to transfected cells with no plasmid indicated that the transfection was successful.

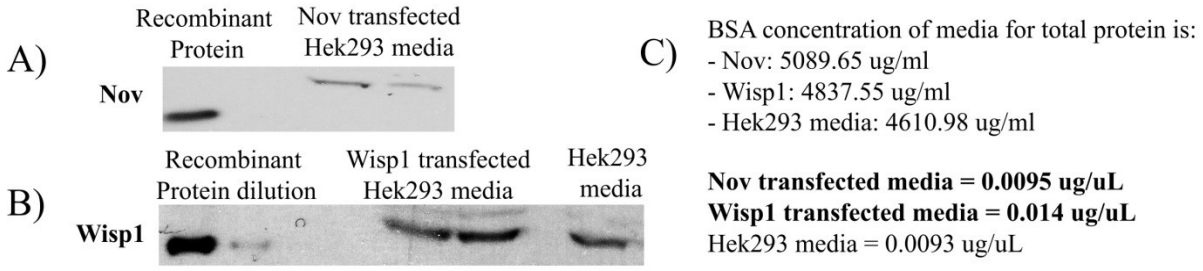

Figure 14. Conditioned Media of Hek293 Cells Transfected with Nov and Wisp1 was Collected After 48 Hours of Culture for Use to Treat Cells *in Vitro*. Using Western blot, the relative concentration used for treatment of cells was determined by comparing transfected Hek293 media to a recombinant protein with known concentration for the specific matricellular protein. **A)** Nov conditioned media concentration was 0.0095 ug/uL determined using a ratio of known recombinant Nov protein (0.5 mg/mL) and **B)** Wisp1 conditioned media concentration is 0.014 ug/uL, determined using a line of best fit approach, using linear regression, created with a dilution of the recombinant Wisp1 protein (0.5 mg/mL). **C)** The BSA assay concentrations and final relative concentrations.

Appendix B – Permissions and Authorizations

Section 1.2. Cardiac Repair and Remodeling Post-MI, Figure 1

This page is available in the following languages: 

Creative Commons License Deed

Attribution-NonCommercial 4.0 International (CC BY-NC 4.0)

This is a human-readable summary of (and not a substitute for) the license.

You are free to:

Share — copy and redistribute the material in any medium or format

Adapt — remix, transform, and build upon the material

The licensor cannot revoke these freedoms as long as you follow the license terms.

Under the following terms:

Attribution — You must give appropriate credit, provide a link to the license, and indicate if changes were made. You may do so in any reasonable manner, but not in any way that suggests the licensor endorses you or your use.

NonCommercial — You may not use the material for commercial purposes.

No additional restrictions — You may not apply legal terms or technological measures that legally restrict others from doing anything the license permits.

Notices:

You do not have to comply with the license for elements of the material in the public domain or where your use is permitted by an applicable exception or limitation.

No warranties are given. The license may not give you all of the permissions necessary for your intended use. For example, other rights such as publicity, privacy, or moral rights may limit how you use the material.